AD-A096 948 LOUISIANA STATE UNIV BATON ROUGE COASTAL STUDIES INST F/6 8/3
DYNAMICS OF FLOW IN THE REGION OF THE TSUGARU STRAIT.(U)
MAR 81 D M CONLON N00014-75-C-0192
UNCLASSIFIED TR-312 NL

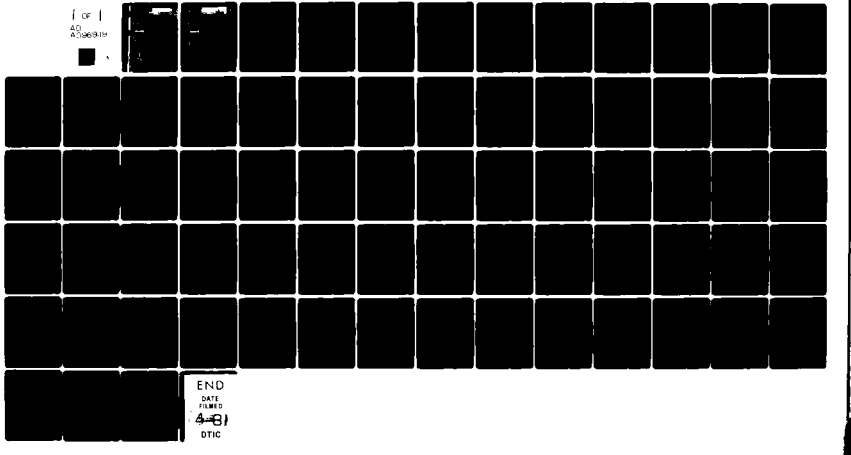

END
DATE FILMED
4-81
DTIC

SEA STRAITS

RESEARCH

Technical Report No. 312

DYNAMICS OF FLOW IN THE REGION OF THE TSUGARU STRAIT

By Dennis M. Conlon

March 1981

Sponsored by:
COASTAL SCIENCES PROGRAM
OFFICE OF NAVAL RESEARCH
ARLINGTON, VIRGINIA 22217

Coastal Studies Institute
Louisiana State University
Baton Rouge, Louisiana 70803

SEA STRAITS

RESEARCH

SSR-1

Technical Report No. 312

DYNAMICS OF FLOW IN THE REGION OF THE TSUGARU STRAIT

By Dennis M. Conlon

Mar[illegible]81

This research is supported by the Office of Naval Research through Contract N000[illegible]4-75-C-[illegible]192 under Project NR 388 002.

Sponsored by

COASTAL SCIENCES PROGRAM
OFFICE OF NAVAL RESEARCH
ARLINGTON, VIRGINIA 22217

Coastal Studies Institute
Louisiana State University
Baton Rouge, Louisiana 70803

ABSTRACT

The Tsugaru Strait is one of four straits that connect the Sea of Japan to adjacent oceans. Flow dynamics in the Tsugaru Strait region are closely tied to the dynamics of the Tsushima Current, a branch of the Kuroshio that enters the Sea of Japan through the Korea Strait and exits through the Tsugaru and Soya Straits. This research concentrates on the dynamic interplay of the Tsushima Current and the Tsugaru Strait in three regions: the inflow region (Sea of Japan side), the strait itself, and the outflow region (North Pacific side).

Dynamic calculations and steric sea leveling in the inflow region indicate that transport into the Tsugaru Strait is principally governed by the geostrophically balanced Tsushima Current. Setup generated south of the strait by the Tsushima Current cannot be maintained at the entrance to the strait; the resulting northward drop in coastal sea level is balanced by a net loss of transport into the strait. Within the strait, the flow is geostrophically balanced in the cross-stream direction. In the longstream direction, the barotropic pressure gradient is chiefly balanced by the longitudinal baroclinic pressure gradient and friction. Application of the Hansen-Rattray (1966) estuarine classification scheme to several straits shows that the Tsugaru Strait displays dynamics similar to that of a well-mixed estuary. The outflow jet emerging from the eastern mouth of the strait is governed by inertial-rotational dynamics; two distinct circulation modes, which behave in a manner consistent with the laboratory findings of Whitehead and Miller (1979), are seen.

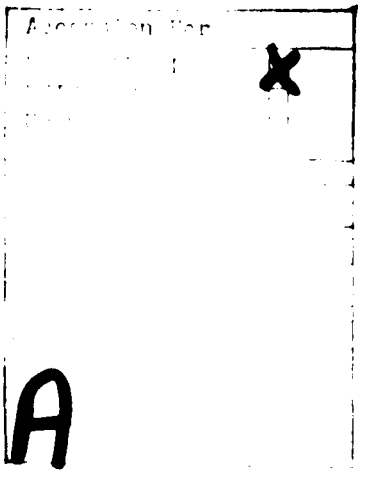

ACKNOWLEDGMENTS

The author extends his sincere thanks to Professor Stephen P. Murray for his continued support and encouragement throughout this endeavor. Helpful comments were also provided during the course of this work by Drs. D. Shoji, C. Sonu, J. D. Thompson, J. Whitehead, J. Suhayda, and T. Ichiye.

Unpublished data were generously provided by Mr. R. Stewart, Mr. K. Nitta, and Mr. R. Peloquin. Professor Y. Nagata and Dr. C. Sonu assisted greatly in securing information and reports from various organizations in Japan. The Japanese Section of the Library of Congress was an invaluable source of information; to Mr. H. Matsumoto and his staff the author extends his special thanks.

Annette A. Conlon performed extensive work in keypunching and data reduction. The figures were drafted by Mrs. G. Dunn and photographed by Mr. K. Lyle. Mrs. M. Mosby typed preliminary versions of the text with diligence and patience. The final text was typed at Coastal Studies Institute.

The Office of Naval Research provided support for a period of extended training at the Coastal Studies Institute, during which time the approach to this research was formulated.

TABLE OF CONTENTS

LIST OF TABLES

LIST OF ILLUSTRATIONS

CHAPTER I

INTRODUCTION

In standard references (e.g., Defant, 1961), one reads that flow in sea straits that connect open oceans with otherwise enclosed marginal seas is principally governed by the characteristics of the water masses produced in the marginal seas. The production of either fresher (evaporation minus precipitation less than zero) or saltier water (E-P>0) in the marginal sea leads to a two-layer exchange with the open ocean in which the net transport in or out is determined by the budget of E-P. The dynamics of the interchange may be further modified by the morphology of the strait.

The theoretical foundation of the dynamics of flow in sea straits, first presented by Defant (1930), has been primarily based on this picture. The emphasis of sea straits research has been oriented toward a fuller understanding of the nature of the steady two-layer interchange, and little attention has been paid to assessing the role of the sea strait in the framework of regional oceanographic processes.

Such a broader view is essential when considering the straits of the Sea of Japan (Fig. 1). This marginal sea of roughly half the area of the Mediterranean is connected with its adjacent oceans by not one but four straits--Tsushima (Korea), Tsugaru, Soya (La Perouse), and Mamiya (Tatar). Of these, only the Mamiya Strait plays a negligible role (Hidaka, 1966). Furthermore, the principal hydrographic feature of the Sea of Japan is not of local origin. The Tsushima Current, a branch of the Kuroshio, passes into the Sea of Japan via the Tsushima Strait and exits through the Tsugaru and Soya Straits (Sverdrup et al., 1942). A low estimate of the transport rate of the Tsushima Current is 2 Sv (1 Sv = 10^6 m^3/sec), while, in comparison, the net transport rate into the Mediterranean, as dictated by the E-P budget, is only about 0.1 Sv (Schott, 1928). It should be expected, then, that the dynamics of flow in the straits of the Sea of Japan might bear little resemblance to the classical mold.

The objective of this paper is to detail the dynamics of flow in the region of the Tsugaru Strait, which is the main outlet of the Tsushima Current as it exits the Sea of Japan. The general problem to be addressed is therefore the interaction between a sea strait and an adjacent boundary current. The general problem will be divided into three parts: the dynamics of inflow of the Tsushima Current into the Tsugaru Strait, the flow dynamics within the strait itself, and the dynamics of the outflow jet which enters the North Pacific Ocean. The principal questions to be asked are:

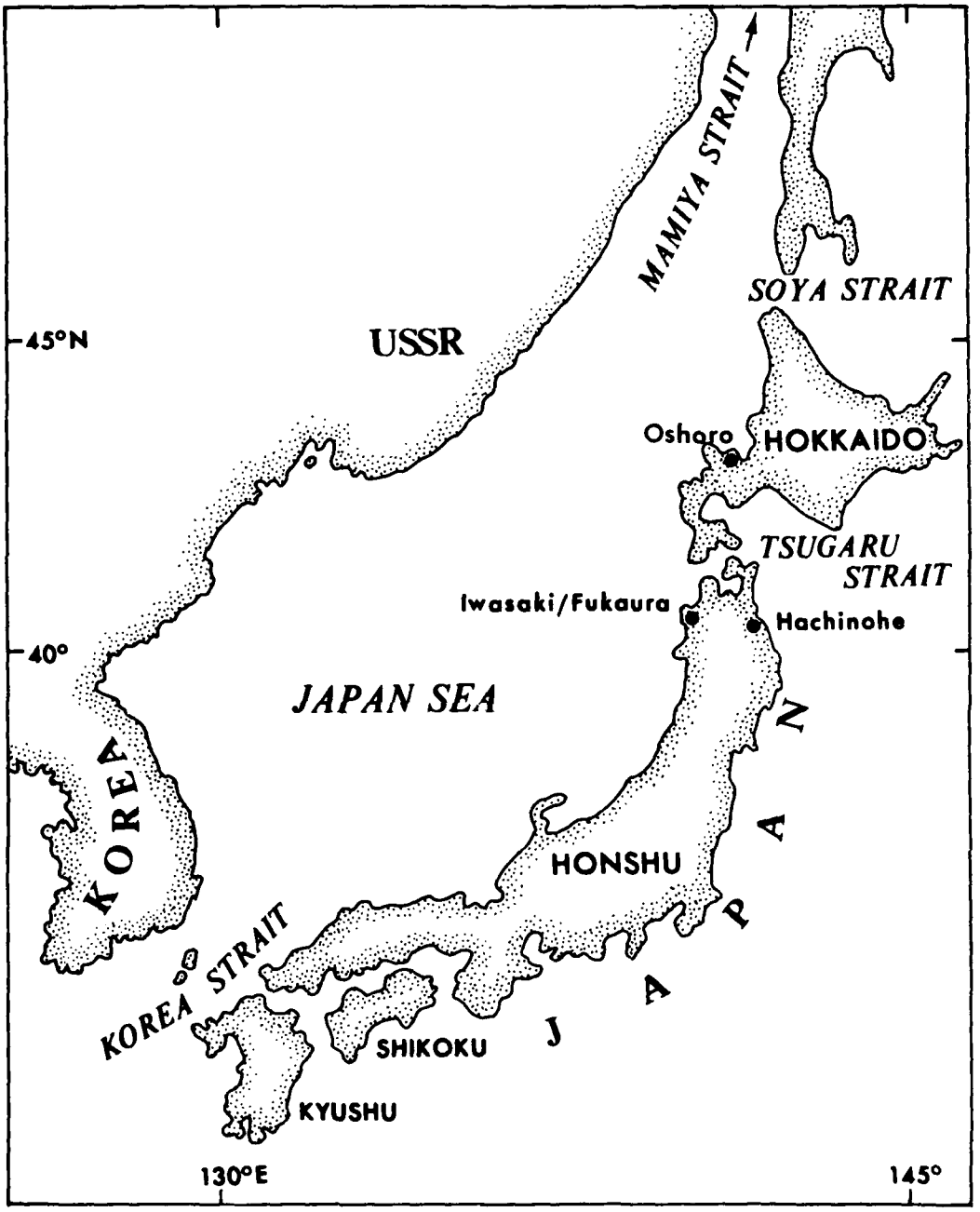

Figure 1. Map of the Sea of Japan.

A. Inflow:

In the inflow region, what is the local momentum balance, and how does the Tsushima Current influence transport into the strait?

B. The Strait:

In several straits of marginal seas, net transport is less than the separate transports of the upper and lower layers. In the Tsugaru Strait, layered flow is undeveloped and net transport is large. How is this reflected in the momentum balance?

C. Outflow:

The water that flows out of the Tsugaru Strait into the North Pacific displays a wide seasonal variability in temperature and salinity. How is this variability reflected in the behavior of the outflow jet?

These questions are addressed using analytical tools tailored to the problems of each regime, and using field data acquired in cruises of various Japanese and United States agencies.

A. Inflow (Chapter IV)

The treatment of the inflow problem begins with a scale analysis of the cross-stream momentum equation for the Tsushima Current. It is shown that the Tsushima Current is in geostrophic equilibrium as it approaches the strait entrance.

Records from current meter moorings in the inflow region show that deep currents (500-m depth and below) are weak, on the order of 2 cm/sec, indicating that calculations based on a level of no motion can be suitably employed. The choice of a deep surface is made by analyzing the vertical variations of the barotropic and baroclinic components of the pressure gradient term across a hydrographic section for which current observations were also made. It is shown that the 400-db surface is an appropriate choice, confirming a historical practice of Japanese researchers.

Using this same reference level, sea level variations in the inflow region are then addressed using steric sea leveling methods (see Chapter III). It is first shown that geostrophic and steric levelings are in close agreement. It is further shown that coastal tide measurements at Iwasaki/Fukaura (adjusted for atmospheric pressure) agree well with steric sea level values obtained at nearby coastal stations, which verifies the earlier work of Nomitsu and Okamoto (1927). The spatial distribution of steric sea level variations is derived for the inflow region to examine the meridional variation in setup induced by the Tsushima Current. A meridional drop in coastal sea level is noted, and is compared with meridional sea level change observed by coastal tide stations. It is thereby hypothesized that a barotropic forcing of flow into the strait may be generated by a loss of setup in the vicinity of the strait. This hypothesis is tested against calculations introduced by Sturges (1968, 1974), whose treatment of the Gulf Stream is contrasted with the present study.

The hypothesis requires that sea level variations be addressed on a regional scale between the Sea of Japan and the North Pacific Ocean. It is known, for example, that sea level at Iwasaki/Fukaura, on the Sea of Japan coast, stands 20 cm higher than at Hachinohe, on the Pacific coast, an amount that is less than the magnitude of the Tsushima Current setup on the Sea of Japan coast. Employing the methods of Lisitzin (1965), it is found that sea level in the far field in the Sea of Japan (~170 km west of the strait) appears to be lower than the corresponding values outside the strait in the North Pacific. This implies that transport through the strait is more likely to be driven by forcing of the entire Tsushima Current system than by density differences across the strait.

B. The Tsugaru Strait (Chapter V)

Flow through the strait is from west to east, and is generally confined to a narrow central core on either side of which are numerous sidewall eddies. The influx of Tsushima Current water through the western narrows is so great that the flow typically does not reverse with depth or in time, despite the existence of strong tidal currents (~2-knot amplitude).

The analysis begins with a scaling of the downstream and cross-stream equations of motion. Previous researchers (e.g., Science and Technology Agency, 1972) have asserted that the downstream balance is between the pressure gradient term and the nonlinear acceleration $u\,\partial u/\partial x$. The treatment in this study, however, indicates that the balance should be between the pressure gradient term and the vertical Ekman term (in Defant's terminology, an antitryptic balance). A solution of the momentum equation is derived for a simple rectangular channel of appropriate dimensions. An analysis is made of each important factor in the solution using available field data. A solution of reduced complexity is derived that is shown to agree well with field observations.

Interestingly, the estuarine circulation/stratification classification scheme of Hansen and Rattray (1966) can be shown to give a satisfactory classification of dynamic variability of various sea straits, including the Tsugaru Strait.

C. Outflow (Chapter VI)

Two distinct modes of outflow circulation exist; they may be designated the coastal mode (colder months) and the gyre mode (warmer months). The water that exits the Tsugaru Strait into the North Pacific typically turns upon leaving the strait, subsequently flowing southward along the Honshu coast to rejoin the Kuroshio (coastal mode). During the warm months of late summer and fall, however, the outflow first circulates around a broad anticyclonic gyre that fills much of the coastal bight south of Hokkaido (gyre mode).

Whitehead and Miller (1979) performed laboratory experiments showing that the coastal and gyre modes are members of a continuum of outflow jet modes distinguished only by the internal Rossby radius of deformation of the jet and topography at the strait exit.

The computed seasonal range of Rossby radii of the outflow jet at the Tsugaru Strait is consistent with the ranges of coastal and gyre modes as hypothesized by Whitehead and Miller.

At the Tsugaru Strait, a transition occurred from gyre mode to coastal mode during December 1975, as verified by data from current meters moored in the outflow region. The time scale of the transition ranges from a minimum of a few days to a maximum of 3 weeks.

D. Data Sources

There are three principal sources of data for the present study. Figure 2 shows the locations of oceanographic stations occupied in October-November 1970 as part of a major oceanographic experiment conducted under the direction of the Japan Meteorological Agency. Considerable benefit was gained by the participation of five oceanographic vessels; for example, the mean length of time to acquire data on Sections A-F was only about 36 hours, thus resulting in a nearly synoptic view of the inflow region. The data acquired during this experiment (hereafter called JMA70) are tabulated in The Results of Marine Meteorological and Oceanographical Observations (Japan Meteorological Agency, 1972, volume 48). A data report on this cruise has been published by the Science and Technology Agency (1972).

Current meter observations and STD station data were acquired during cruises of the USNS SILAS BENT in the Tsugaru Strait region (Fig. 3). These heretofore unpublished data were provided through the courtesy of R. A. Peloquin and O. Smith of the U.S. Naval Oceanographic Office.

A 3-year study of currents and tides in the Tsugaru Strait region was conducted in 1975-77 under the direction of the Japan Maritime Safety Agency (Fig. 4). A data report on this experiment has been published by the Science and Technology Agency (1979). Unpublished field data have been provided courtesy of Professor Y. Nagata and Mr. K. Nitta. This experiment will be referred to as JMSA75.

Additional hydrographic data and tide data were obtained from the following sources:

Results of Marine Meteorological and Oceanographical Observations, Japan Meteorological Agency

Hydrographic Bulletin, Japan Hydrographic Office

Results of Tidal Observations, Japan Maritime Safety Agency

Data Report of Oceanographic Observations, Japan Maritime Safety Agency

Meteorological Observations, Japan Meteorological Agency

Tidal Observations, Japan Geographical Survey Institute

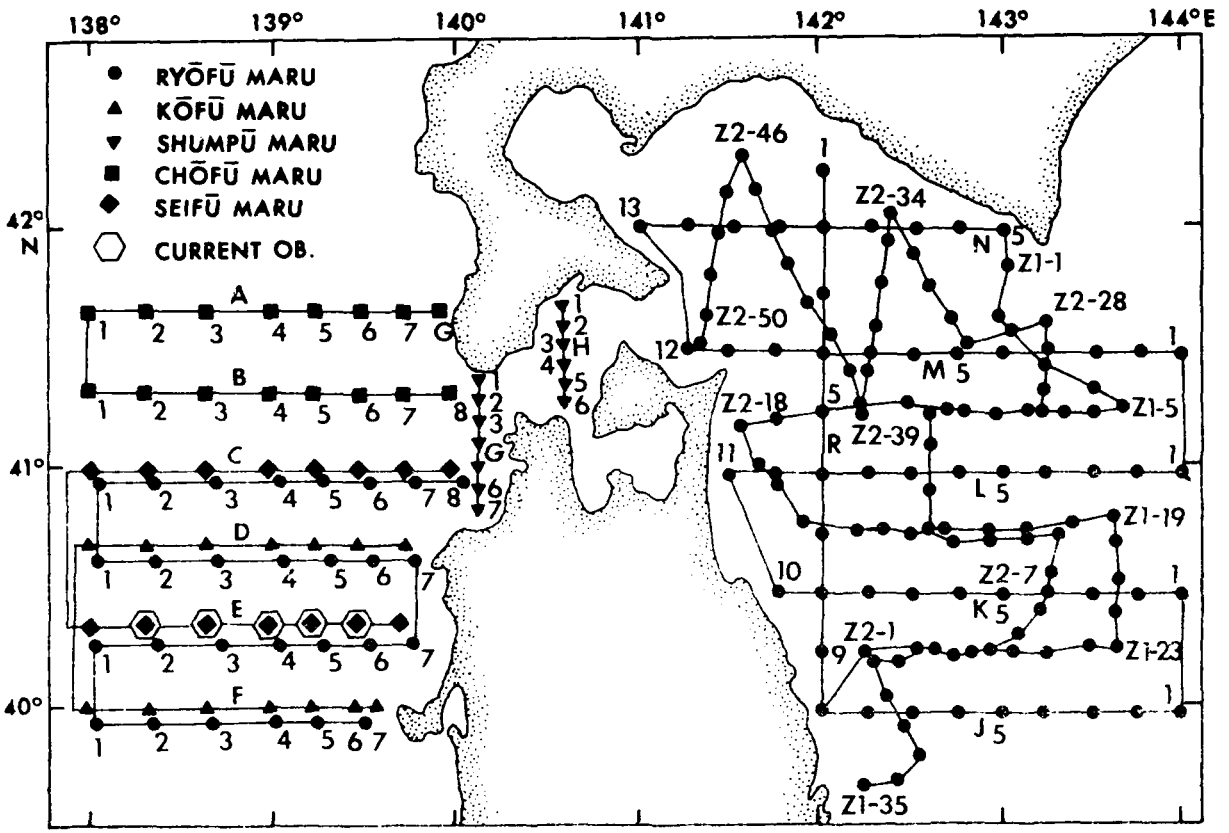

Figure 2. Survey lines of Japanese multi-agency experiment JMA70 in Tsugaru Strait region. Stations with z prefix = BT, GEK only, hydrographic casts at all other stations; current observations at stations CM1-5.

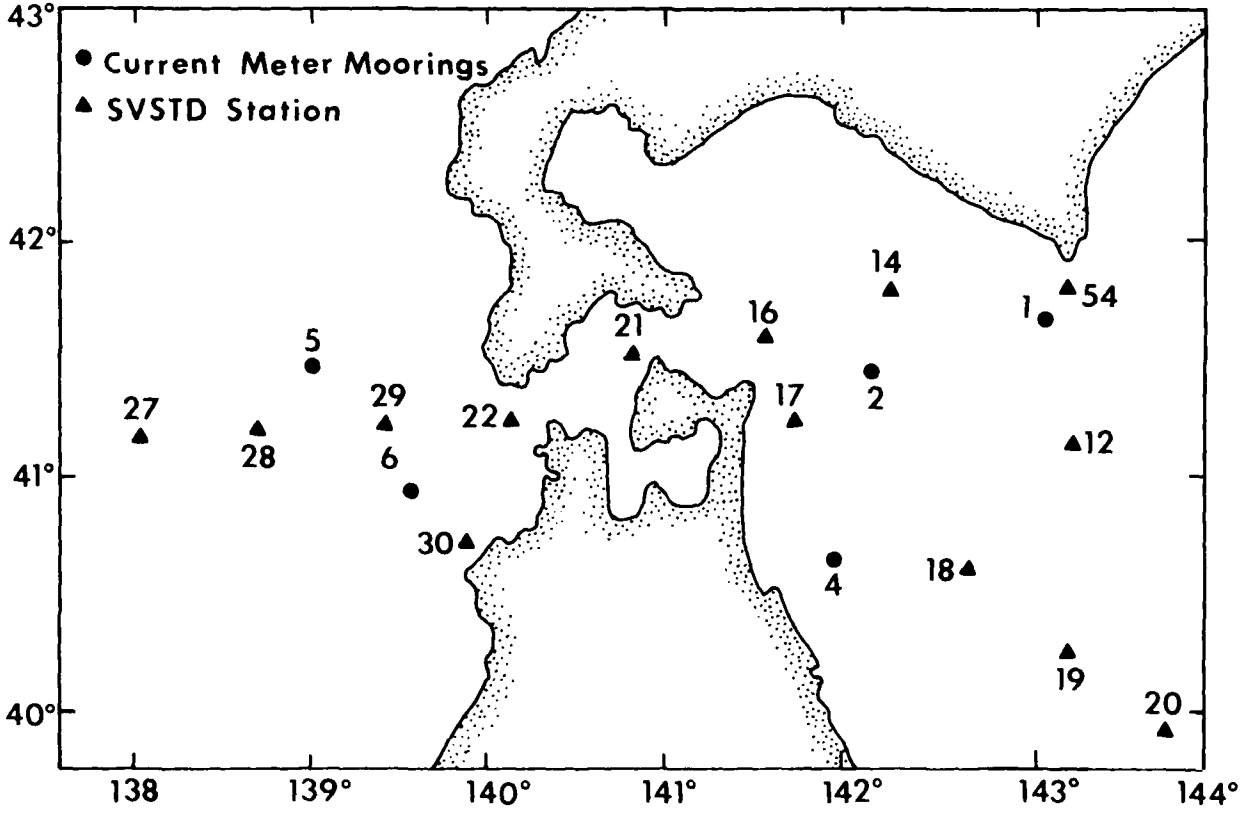

Figure 3. Locations of current meter moorings and SVSTD stations, cruises of USNS SILAS BENT, November 1975 and January 1976.

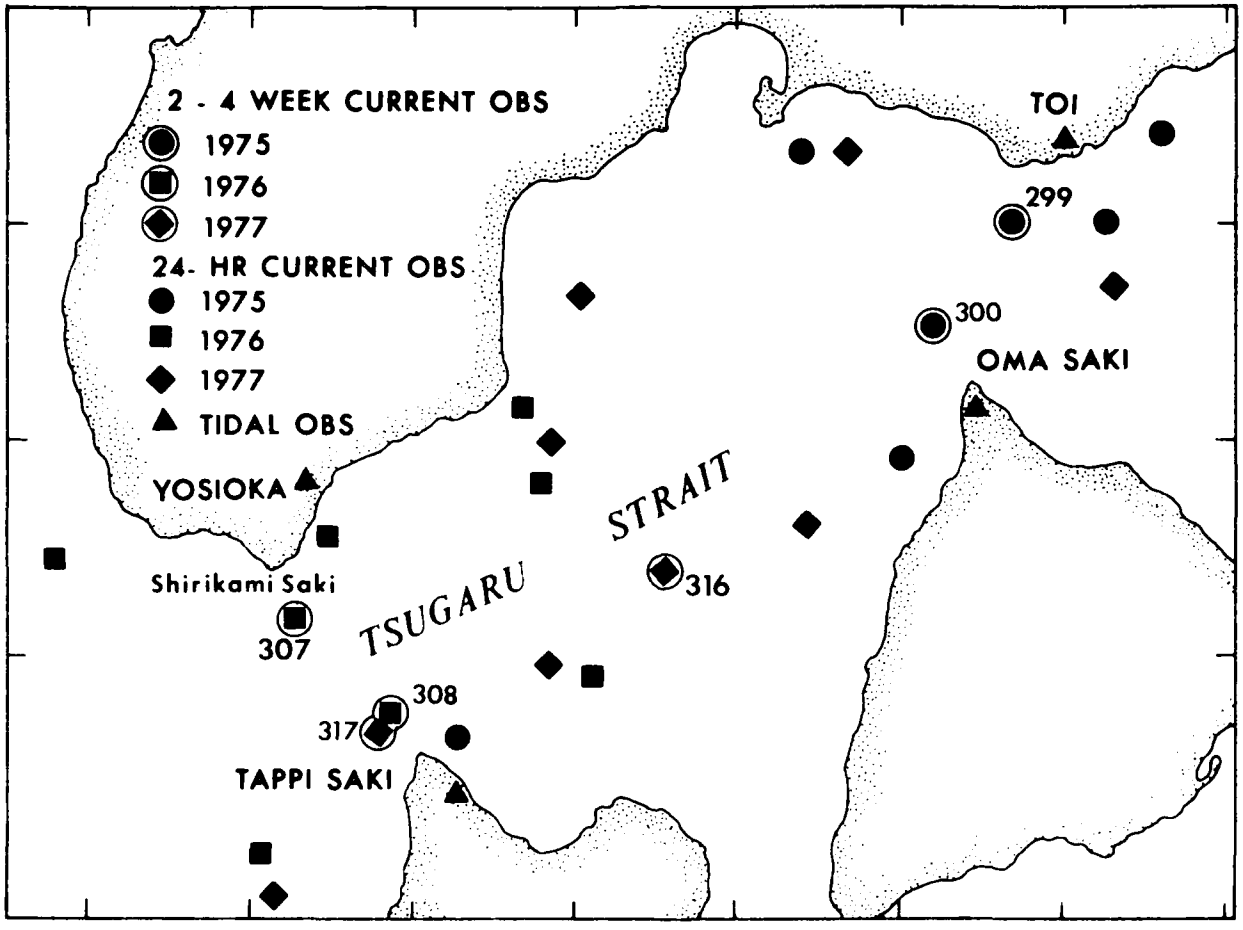

Figure 4. Locations of current meter observations and tidal stations, JMSA75 (October-November 1975; September 1976; July 1977).

CHAPTER II

THE SEA OF JAPAN AND THE TSUSHIMA CURRENT

A. Water Masses of the Sea of Japan/Tsushima Current

The Sea of Japan is an adjacent sea roughly half the size of the Mediterranean. It is connected to its adjacent ocean by four straits: Korea (Tsushima), Tsugaru, Soya (La Perouse), and Mamiya (Tatar). The maximum depth of free communication with the adjacent ocean is 150 m (sill depth of Korea Strait), while the mean depth of the Sea of Japan is nearly 1,500 m. Because of this limited connection, the intense winter cooling in the northern part of the Sea of Japan serves to produce deep and bottom water of remarkable uniformity (Suda et al., 1932; Moriyasu, 1972; and others). Yasui et al. (1967) estimate that nearly 90% of the water of the Sea of Japan has a temperature of 0-1°C and salinity of 34.0-34.1 $^{o}/_{oo}$. Defant (1961, p. 129) has pointed out that such uniformity of deep water is a common feature of adjacent seas which are subject to winter convection and which have limited connection to their adjacent oceans; similar conditions exist in the Mediterranean and the Red Seas.

Riding over this cold, uniform mass of water is the major current of the Sea of Japan, the Tsushima Current, a branch of the Kuroshio, which enters through the Korea Strait, moves along the west coast of Japan, and then exits through the Tsugaru and Soya Straits (Fig. 5). From late fall to early spring, the Tsushima Current brings water of high temperature (8-15°C) and high salinity (~34.4-34.5 $^{o}/_{oo}$) into the Sea of Japan. From late spring to early fall, this water of Kuroshio origin is augmented by water of East China Sea/Yellow Sea origin, characterized by very high temperatures (greater than 20°C) and low salinity (32-34 $^{o}/_{oo}$).

Thus there are three principal water masses that must be considered in order to characterize the Tsushima Current in the Sea of Japan. Figure 6 is a hydrographic section obtained by the KOFU MARU during JMA70 (Section D, lat. 40°40' N; October 15, 1970). In this section, the Tsushima Current is observed east of longitude 139° east down to a depth of about 200 m. The water of East China Sea origin is easily recognized by its high temperature (>20°C) and low salinity (<33.6 $^{o}/_{oo}$). Below 50 m is water of Kuroshio origin, roughly outlined by the 34.2 $^{o}/_{oo}$ isohaline. Below 300 m (100 m at long. 138° E) lies the uniform Sea of Japan deep water.

B. Path of the Tsushima Current

After entering through the Korea Strait, the Tsushima Current branches and meanders within the Sea of Japan in a complex sequence of

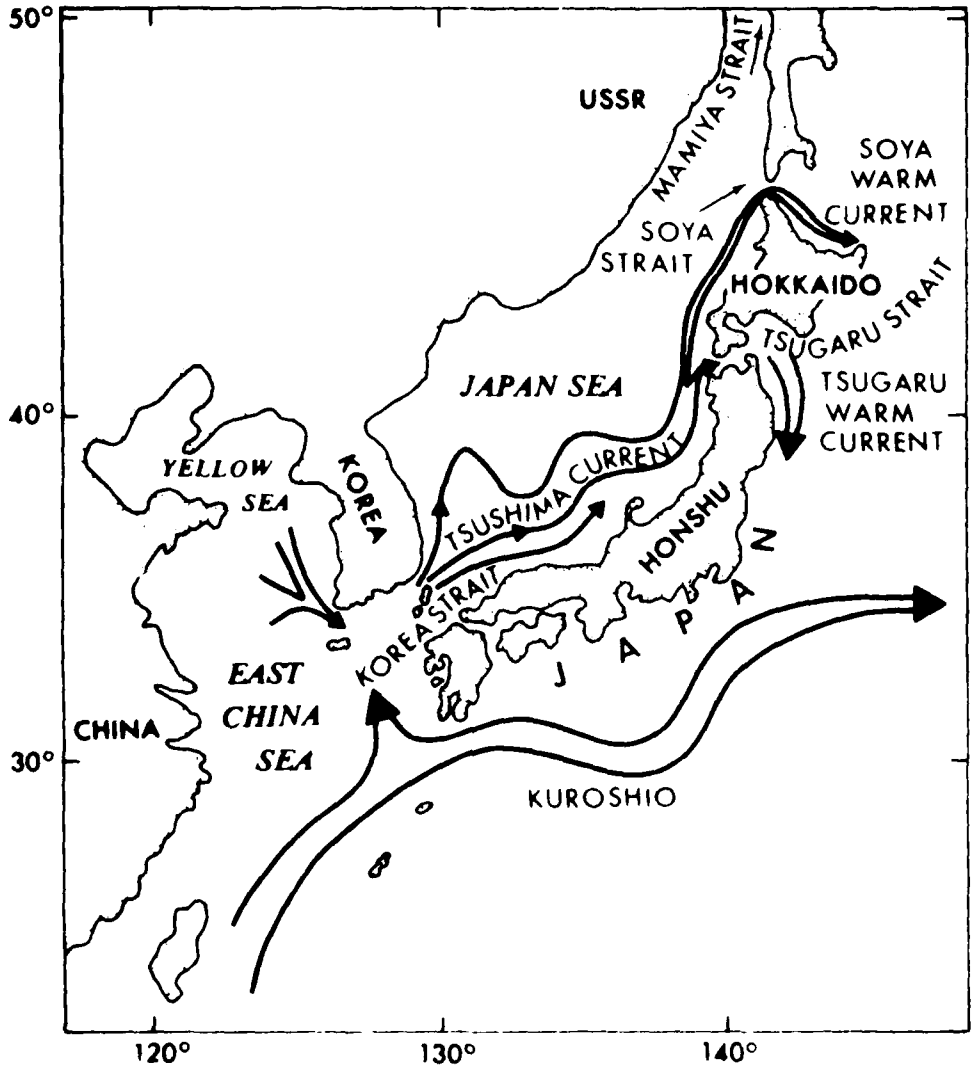

Figure 5. Map of East China Sea/Japan Sea showing Kuroshio System, consisting of Kuroshio, Tsushima Current, Tsugaru Warm Current, Soya Warm Current.

maneuvers (Fig. 5). A western component, the East Korean Warm Current, flows northward along the Korean coast with a transport rate of more than 1 Sv, but about 90% of this current flows back to the south and southeast to recombine with the eastern components of the Tsushima Current (Tanioka, 1968). There are two or three eastern components (a subject of much debate) that flow along the coast of Japan in large meanders in which distinct warm (cold) water masses are found in regions of anticyclonic (cyclonic) shear. The positions of the meanders appear to be topographically controlled (Fukuoka, 1957). This meandering generally ceases at latitude 40° north, at which point the Tsushima Current has been reformed into a single component flowing toward the north near the

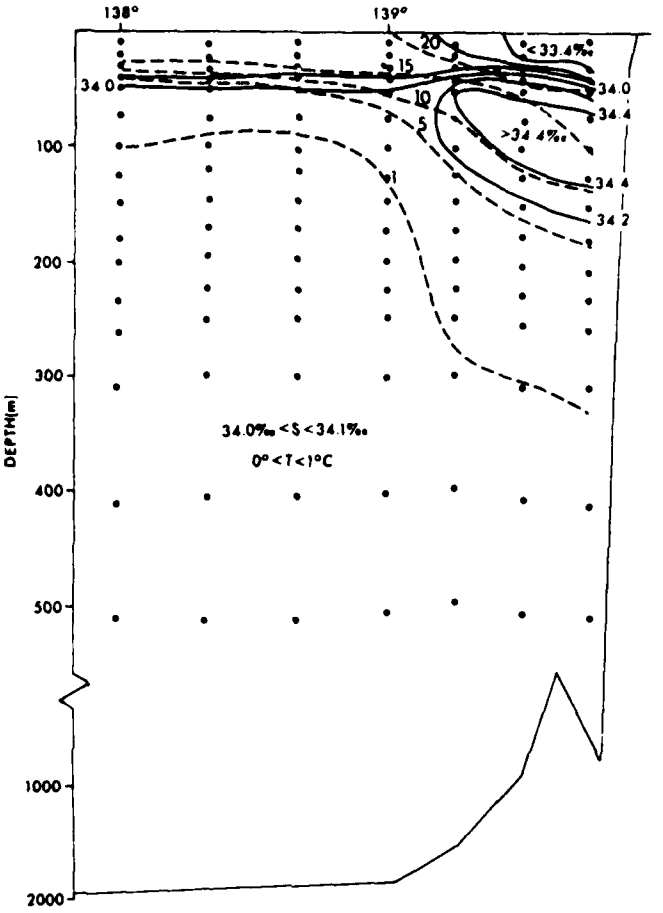

Figure 6. Hydrographic section on latitude 40°40'N from cruise of KOFU MARU, October 15, 1970 (Section D, Run I, JMA70), showing Tsushima Current inshore of longitude 139°E. Warm (T>20°C), low-salinity (S<33.6 °/$_{oo}$) water is of East China Sea origin; Kuroshio water roughly outlined by S = 34.2 °/$_{oo}$ isohaline.

Honshu coast south of the Tsugaru Strait.

Most of the Tsushima Current flows out of the Sea of Japan through the Tsugaru Strait, while the remainder flows along the Hokkaido coast and out through the Soya Strait (Moriyasu, 1972). Hata (1962) performed geostrophic calculations of volume transport through hydrographic sections obtained during 1947-1961 on lines 41°N and 42°N (i.e., bracketing the Tsugaru Strait) and found that between 50% and 100% of the northward transport of the Tsushima Current was diverted into the Tsugaru Strait. He computed the range of volume transport of the Tsushima Current to be 2-7 Sv, with a minimum transport in winter and a maximum transport in fall. Of this transport, between 1 and 4 Sv flowed into the Tsugaru Strait.

The dramatic diversion of Tsushima Current flow into the Ts garu Strait will be the focal point of the analysis in Chapter IV.

CHAPTER III

STERIC SEA LEVELING

In Chapter IV, on the inflow region, a great deal of emphasis is placed on determining sea surface topography by steric sea leveling. It is therefore appropriate to devote some attention to the theoretical basis of the technique. [More complete derivations can be found in Pond and Pickard (1978) and other standard texts.]

A level surface is a surface on which the potential energy of a mass remains constant. Level surfaces are therefore surfaces of constant gravitational potential, or geopotential ϕ, defined by

$$g \equiv \partial\phi/\partial z \tag{1}$$

If one raises or lowers a unit mass by a distance h, the work done is $\pm gh$, and the unit mass now rests on an equipotential surface of higher or lower gravitational potential ($\pm d\phi$). Conversely, two equipotential surfaces that differ in geopotential by some quantity $d\phi$ are a vertical distance $d\phi/g$ apart.

Now the mass distribution in the ocean can be completely specified by the distribution of either density or specific volume. The relationship between geopotential and the mass distribution can be obtained by combining equation (1) with the differential form of the hydrostatic equation

$$\alpha dp = g dz$$

to obtain

$$\alpha dp = g \frac{\partial\phi}{\partial z} dz, \tag{2}$$

which can be integrated between (z_1, p_1) and (z_2, p_2) to obtain

$$\int_{p_1}^{p_2} \alpha dp = \phi_2 - \phi_1 = \Delta\phi \tag{3}$$

where $\Delta\phi$ is called the geopotential distance (units of energy per unit mass).

The field of specific volume $\alpha s,t,p$ is composed of an invariant field $\alpha 35,0,p$ and a variant field δ (the anomaly of specific volume). The mass distribution in the ocean can therefore be specified by the field of δ alone. Likewise, the geopotential distance $\Delta\phi$ consists of an invariant term ϕ_s (derived from the invariant field $\alpha 35,0,p$) and a variant field ϕ_a, called the geopotential anomaly; that is, equation (3) reduces to

$$\int_{p_1}^{p_2} \delta \, dp = \phi_a \tag{4}$$

In practice, the integration of (4) extends from the surface to some deep reference surface. At the surface, we take $p_1 = 0$; atmospheric pressure is assumed constant and is therefore neglected. If the deep isobaric surface p_2 is a level surface, then (4) will yield an absolute topography of the sea surface. In a given ocean region, two locations that differ in geopotential anomaly by $\Delta\phi_a$ (referenced to p_2) will differ in height by $\Delta\phi_a/g$. This method of calculating an absolute topography of the sea surface is called steric sea leveling.

Perhaps the most crucial factor in assessing the adequacy of steric leveling results is a determination of the slope of the deep pressure surface. Ideally, the deep pressure surface should be a level surface. In practice, deep currents below the reference surface are almost always present, and these currents produce a slope of the deep isobaric surface. Hence, in Chapter IV attention is devoted to assessing deep flow in the inflow region (Section IV-C), the choice of a suitable reference surface (Section IV-D), and the slope of the reference surface in the inflow regime (Section IV-E).

Even if the deep pressure surface is a level surface, there are other effects that can alter sea surface topography and yet not appear in steric leveling results. They are atmospheric pressure variations, setup by onshore winds, and river discharge effects (Sturges, 1967). Of the factors, the influence of river outfall in the inflow region can be quickly dispensed with. The largest river of this region is the Yoneshiro, which has a maximum discharge in the spring of less than 10^3 m^3/sec. The mean sea level at Iwasaki is at a minimum in the spring (see Fig. 9), so it appears highly improbable that freshwater discharge has any appreciable effect.

The effects of wind setup appear to be likewise of second-order importance. Given an onshore wind stress τ, the total rise in Δh in sea level between a point X offshore and the coastline is given by

$$\Delta h = \frac{\tau\alpha}{g} \int_{-x}^{o} \frac{1}{D} \, dx$$

where D is the depth of the water, and where bottom stress is neglected. The maximum monthly onshore wind stress in the inflow region is about 1 $dyne/cm^2$ in January (Hidaka, 1958). Such a wind blowing across the Sea of Japan ($X \sim 10^3$ km, $D \sim 1.5 \times 10^3$ m) would produce a setup of slightly

more than 0.5 cm. In addition, the maximum shelf width of the inflow region is about 50 km (vicinity of Tsugaru Strait), but depths are uniformly greater than 100 m. For X = 50 km and D = 100 m, Δh again is about 0.5 cm, thus giving an estimate for total wind effect of about 1 cm, a negligible value. Of course, for intense, short-term events such as severe storms, wind setup may reach many centimetres, and such an effect would be appreciable. Such events, however, are not within the scope of the present analysis.

Atmospheric pressure variations will induce sea level changes via the inverse barometric effect, which is approximated as 1 cm of sea level change per 1 mb of atmospheric pressure change. Atmospheric pressure values are well known for the study area, and no difficulty arises in making suitable corrections. It should be noted, however, that when comparing coastal tide measurements to offshore steric leveling results (e.g., Section IV-E.2), one must never "correct" steric measurements for atmospheric pressure. In steric sea leveling, the surface is taken to be isobaric. Rather, one should correct coastal tide measurements for atmospheric pressure before comparing to steric leveling results.

CHAPTER IV

THE INFLOW REGION OF THE TSUGARU STRAIT

A. Introduction

In this chapter an attempt is made to detail the essential dynamics of the Tsushima Current in the vicinity of the Tsugaru Strait. The mechanisms of generation of the Tsushima Current are not treated, but rather attention is given to the current as an input condition for the limited area under consideration, which extends roughly from 40°N to 42°N.

On this scale a simple working hypothesis can be formulated as follows. As the Tsushima Current moves northward along the Japan coast, sea level will be elevated at the coast because of the influence of the Coriolis acceleration. When the current encounters the Tsugaru Strait, however, this setup cannot be maintained and a significant readjustment of the flow must take place. Hypothetically, this readjustment should result in a forcing of flow into the strait.

B. Cross-Stream Momentum Balance of the Tsushima Current

Using a coordinate system in which x points east, y north, and z downward, the momentum equation in the x direction for steady-state, inviscid flow is

$$u\frac{\partial u}{\partial x} + v\frac{\partial u}{\partial y} + w\frac{\partial u}{\partial z} = -\frac{1}{\rho}\frac{\partial p}{\partial x} + fv + A_x\frac{\partial^2 u}{\partial x^2} + A_y\frac{\partial^2 u}{\partial y^2} + A_z\frac{\partial^2 u}{\partial z^2} \qquad (5)$$

where f is the Coriolis parameter and A_i = eddy viscosity in direction i.

The characteristic width and depth scales for the Tsushima Current are X = 50 km and Z = 100 m. The scale of Y is 100 km, which is roughly the downstream length scale of the turning process. Characteristic velocities are u = 10 cm/sec and v = 50 cm/sec and vertical motion will be neglected. For A_x and A_y a value of 10^8 cm^2/sec is used, and $A_z = 10^3$ cm^2/sec. While these eddy viscosity estimates are in the high range of values normally used, they are not inappropriate for coastal flow (Officer, 1976); furthermore, liberal estimates should prevent an unwarranted disregard for frictional effects.

With these scaling parameters, the order of magnitude of the terms in (5) are (cgs units):

$$2 \times 10^{-5} + 5 \times 10^{-5} + 0 = -\frac{1}{\rho}\frac{\partial p}{\partial x} + 5 \times 10^{-3} + 4 \times 10^{-5} + 10^{-5} + 10^{-4}$$

Therefore, to within a few percent the momentum balance should be in geostrophic equilibrium.

I wish to test the accuracy of the geostrophic approximation against field data acquired during JMA70. Current observations were made during a 30-hour period on October 10-11 at four levels (10 m, 50 m, 100 m, 200 m) at stations CM1-CM5 (Fig. 2). Profiles of salinity and temperature were also taken at CM1 and CM5 just before and just after the current meter observations. There is, however, one difficulty with the current observations: the measurements were made using a "two current meter" technique in which one meter was kept at a depth of 500 m and the other was placed sequentially at the four upper levels. If there were no motion at 500 m, the deep meter would yield ship drift and thus provide a correction for the upper meter. Unfortunately, there was no direct measurement of flow at 500 m.

C. Deep Flow in the Sea of Japan

Direct measurements of deep flow in the Sea of Japan are exceedingly scarce. The only literature reference on the subject found was that of Nan-niti et al. (1966), who used a neutrally buoyant float to measure currents at 800 m in the western Sea of Japan. They found inertial oscillations of 3.5 cm/sec superimposed on a mean flow of 1.5 cm/sec.

Indirect measurements of flow at 500 m can be made by geostrophic calculations based on a much deeper reference level. Ohwada and Tanioka (1972) calculated currents at the 500 db level referenced to 1,000 db and found a maximum current of 3 cm/sec in the eastern Sea of Japan. They also calculated flow at 1,000 db based on a 1,200-db level and found a maximum current of about 2 cm/sec.

Fortunately, a recent survey by the U.S. Naval Oceanographic Office has provided data that give us the best information to date on deep flow in the Sea of Japan. Moored current meters were deployed during November 1975-January 1976 at two locations near the western entrance to the Tsugaru Strait (Fig. 3). In Figure 7, 72-hour averaged currents at station 6 (546-m depth) and station 5 (442 m) are shown. The currents at station 5 are quite weak; both u and v have a maximum value of about 2 cm/sec. Currents at station 6 are somewhat less weak. The values of u reach peaks of $\pm$ 3-4 cm/sec; values of v are generally less than $\pm$2 cm/sec, but for a brief time reach 6 cm/sec. As a general approximation of flow at these depths, however, it is reasonable to estimate the deep flow as about 2-3 cm/sec with a highly variable direction. While such measurements do not exist for JMA70, we nonetheless have an order of magnitude estimate of the error incurred in assuming no motion at a deep reference surface.

D. Geostrophic Balance of the Tsushima Current

We begin with the geostrophic equation

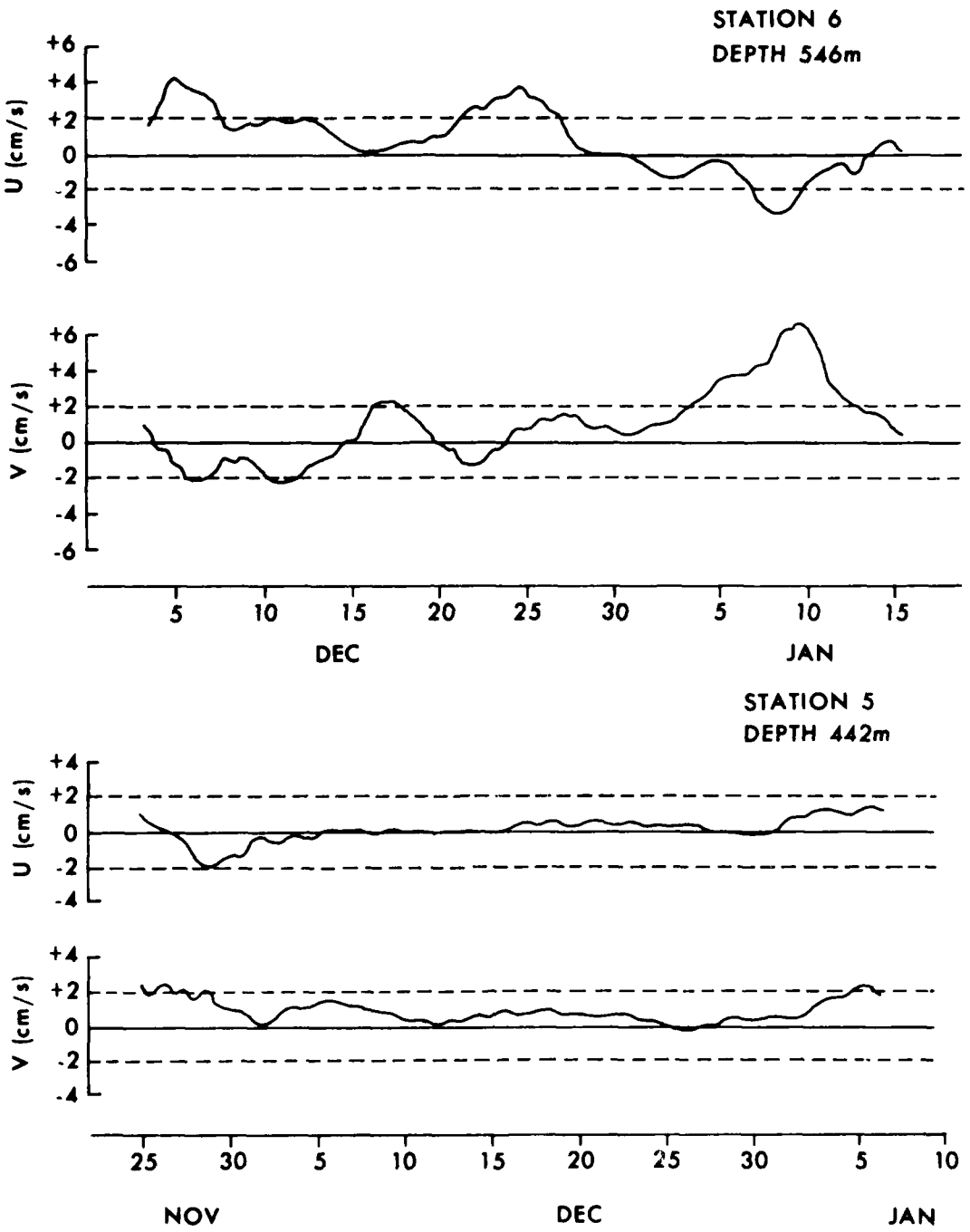

Figure 7. Deep currents in the inflow region, November 1975-January 1976. For locations of current meters, see Figure 3.

$$\frac{1}{\rho}\frac{\partial p}{\partial x} = fv$$

and by setting

$$p = p_a + g\int_{\zeta}^{z} \rho(x,z)\, dz ,$$

where p_a is the atmospheric pressure and ζ is the elevation of the sea surface (positive downward). Using Leibnitz' Rule, differentiation yields

$$\frac{\partial p}{\partial x} = \frac{\partial p_a}{\partial x} - g\,\rho_s\frac{\partial \zeta}{\partial x} + g\int_{o}^{z}\frac{\partial \rho}{\partial x}\, dz \qquad (6)$$

where the integration limit at the surface is taken to be zero without appreciable loss of accuracy and ρ_s is the surface density (Officer, 1976). The geostrophic balance is then

$$0 = -\frac{1}{\rho}\frac{\partial p_a}{\partial x} + g\frac{\partial \zeta}{\partial x} - \frac{g}{\rho_c}\int_{o}^{z}\frac{\partial \rho}{\partial z}\, dz + fv \qquad (7)$$

where ρ_c is the mean density of the water column from the surface to depth z.

During JMA70 measurements of atmospheric pressure were made each time a hydrographic cast was made. The maximum atmospheric pressure gradient measured was on the order of 10^{-7}, which is several orders of magnitude less than fv (order of 10^{-3}). The first term on the right-hand side of (7) can be neglected. The remaining terms in the momentum equation (7) are:

$$0 = g\frac{\partial \zeta}{\partial x} - \frac{g}{\rho_c}\int_{o}^{z}\frac{\partial \rho}{\partial x}\, dz + fv. \qquad (8)$$

Note that the barotropic term pointing westward (sea level rising toward the coast) is balanced by the Coriolis term (v northward) and the baroclinic term (lighter water toward the coast), which point eastward.

At the surface the baroclinic term vanishes, so that the barotropic term can be calculated using the measured values of surface currents between stations CM1 and CM5. The baroclinic term can be easily calculated from the hydrographic casts made at CM1 and CM5. The results of applying (8) to the section CM1-CM5 are shown in Figure 8a-b. In performing this calculation, the currents measured at 10 m were taken to be representative of surface values. The velocities at each of the four levels are time-averaged, sectionally averaged means. Figure 8a shows the balance of momentum terms using the hydrographic casts made just prior to the current observations, and Figure 8b uses the casts made just after. Note that in Figure 8a the momentum terms at each of the four levels balance within about 10%, while the agreement shown in Figure 8b is within about 5%. A neglected deep flow of $\pm$ 2 cm/sec would alone produce an uncertainty of nearly 10%, and so we can conclude that the flow is in geostrophic equilibrium within the errors of observation.

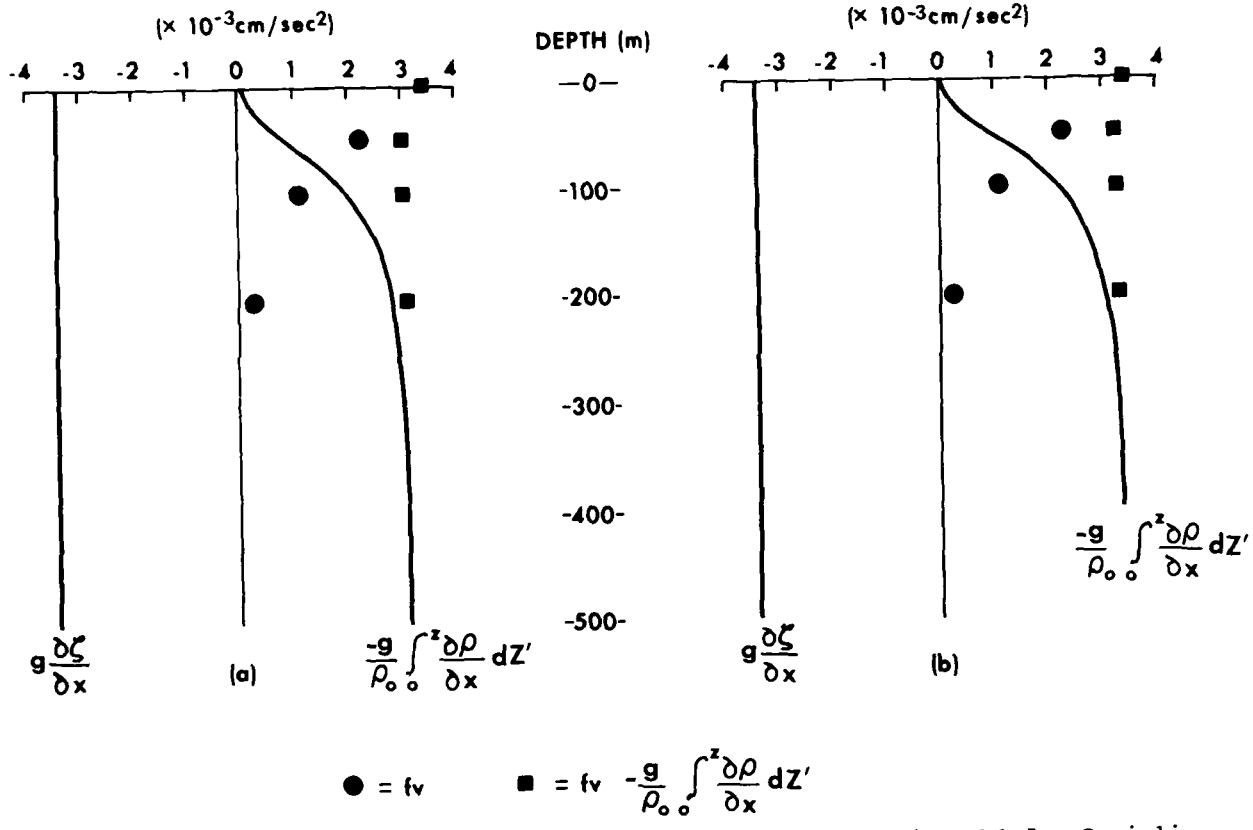

Figure 8. Vertical variation of cross-stream balance on section CM1-5. Coriolis term calculated from current meter observations; barotropic term calculated using slope derived from mean surface currents; baroclinic term calculated from hydrographic casts made (a) before and (b) after current observations.

An examination of Figure 8a-b also reveals other useful information. First, the baroclinic current (i.e., the Tsushima Current) is substantially confined to the upper 200 m of the water column. Second, the baroclinic pressure gradient is within 1% of its limiting value at 400 m. Subject to the uncertainty of deep flow, 400 db appears to be an excellent reference level for geostrophic calculations of volume transports. Japanese investigators have often used a 400-db reference level for volume transport calculations of the Tsushima Current (e.g., Hata, 1962), and the above considerations provide a verification of that choice.

E. Steric Sea Leveling in the Inflow Region

1. A comparison of geostrophic and steric leveling. The establishment of an adequate deep reference surface also provides the possibility of measuring sea level variations by steric methods (see Chapter III). To illustrate this point, we again consider the data obtained for stations CM1-CM5.

Following Sturges (1974), we first take the geostrophic equation at $z = 0$,

$$fv = -g \frac{\partial \zeta}{\partial x} ,$$

and integrate over the distance between stations to obtain the finite difference form

$$\Delta h = \frac{f}{g} \langle v \rangle X \qquad (9)$$

where $\langle v \rangle$ is the average velocity over a separation distance X and Δh is the cross-stream change in sea level, now measured positive upward.

Over the 30-hour period of current observations, a mean surface current of $\langle v \rangle = 36$ cm/sec was measured between stations CM1 and CM5, which were separated by a distance of 85 km. The change in sea level between these stations should, according to (9), be $\Delta h = 29$ cm. Montgomery (1969) calls this geostrophic leveling.

The hydrographic data obtained at CM1 and CM5 can also be used to calculate steric sea level change between these stations via equation (4). Immediately prior to the current observations, the calculated rise in steric sea level (0/400 db) was $\Delta h_{st} = 27$ cm; just after the observations were completed, the value was $\Delta h_{st} = 29$ cm. As before, the geostrophic leveling is subject to error induced by neglecting deep flow, and a deep current of ± 2 cm/sec would throw the geostrophic leveling result off by about ± 2 cm. Within the accuracy obtainable, then, steric sea leveling and geostrophic leveling are in excellent agreement.

2. Steric sea leveling compared to a coastal tide station. The comparison of coastal tide data to offshore steric leveling in the Sea of Japan has been the subject of a number of earlier studies (e.g., Nomitsu and Okamoto, 1927; Miyazaki, 1955; Patullo et al., 1955; Yi, 1967; Lisitzin, 1967). These previous investigations agree on three principal

points: (1) in the Sea of Japan, steric variations are the primary cause of coastal sea level changes, while (2) barometric pressure has a secondary effect and (3) wind has almost no effect.

Of these previous works, only Nomitsu and Okamoto (1927) treat steric variations near the inflow region of the Tsugaru Strait. In their study, mean monthly sea level and barometric pressure at Iwasaki (see Fig. 1) were correlated with offshore steric variations. While they reached the same three conclusions as noted above, there were several problems with their study. First, the offshore data were acquired nearly 100 km to the south of Iwasaki; as will be seen in the next section (cf. Fig. 10), the extreme meridional variations in sea level in the inflow region suggest that such data may have been acquired too far from the coastal station. Second, the steric data were based on measurements at only four levels: 0 m, 50 m, 100 m, and 200 m; such data can be expected to only poorly resolve the steric contributions from the upper layer structure. Third, the deepest density measurement was at 200 m; while Figure 8 suggests that the baroclinic part of the current is largely limited to 200-m depth, a deeper set of measurements would have been more appropriate. Finally, Nomitsu and Okamoto used barometric pressure variations to correct the steric measurements, rather than the coastal tide data; as pointed out in Chapter III, this is theoretically unjustified.

In an attempt to verify the work of Nomitsu and Okamoto, I have correlated tidal variations and barometric pressure variations at Iwasaki/Fukaura with offshore steric heights for the period 1956-1976. I place two limitations on the use of steric data. First, the hydrographic casts had to extend to 400 db. Second, I limited the area in which the casts were made to a region bounded by latitude 40°35'-40°40' north, longitude 139°40'-139°45' east. The distance between any station and Iwasaki/Fukaura was typically 5-7 km. Because the adjacent shelf drops off so sharply in this area, no shallow water corrections were necessary. Because of the above limitations, only 21 appropriate stations were located, and they were occupied in only 6 of the 12 months. This scarcity of data led me to use the entire 1956-76 record of tides and barometric pressures, rather than limit myself to such data as were acquired only when stations were occupied.

The results of such a correlation are presented in Figure 9 a-c in the style of Reid and Mantyla (1976). Mean values and standard deviations of coastal sea level and barometric pressure are shown in Figure 9a and 9b. Means of steric heights (0/400 db) are shown in Figure 9a and are correlated with sea level corrected for barometric pressure in Figure 9c. The left ordinate (for tides and barometric pressure) is expressed in deviation from the mean for 1956-76. The right ordinate is in length units. The February value of steric height is from one station; all other stations are the means obtained from 2-7 stations. Note that for 5 of the 6 months tested the agreement between steric values and corrected coastal data is extremely close, while the agreement in March is within the standard deviation of measured coastal sea level. Again, we see a demonstration of the efficacy of steric leveling.

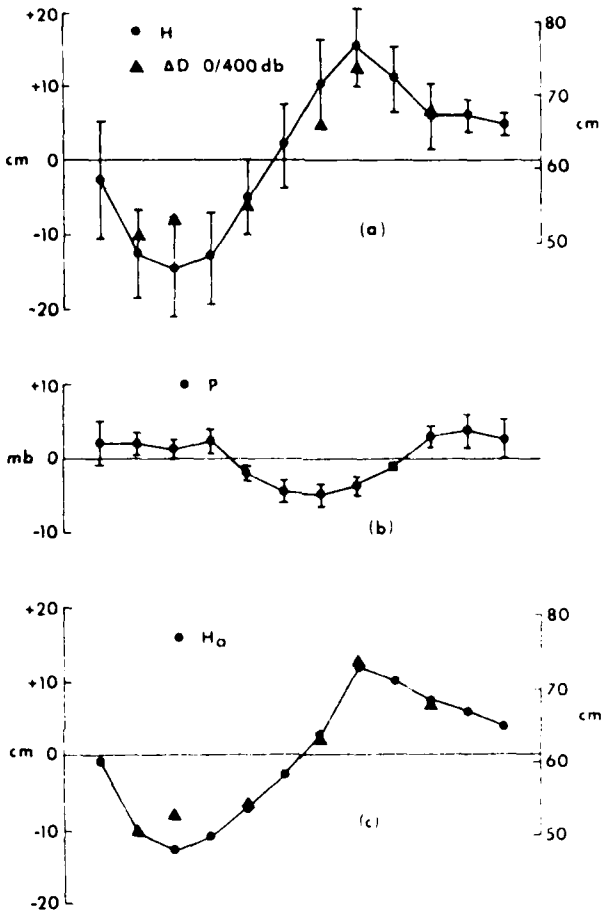

Figure 9. Seasonal sea level variations (January-December) at Iwasaki/Fukaura. (a) Departures of the monthly mean tide gauge record from the annual mean for 1956-1976 and monthly mean steric height for 1957-1975. Bars indicate standard deviation. (b) Atmospheric pressure departures with standard deviations. (c) Tide gauge departures adjusted for atmospheric pressure and steric heights.

F. Shape of the Sea Surface in the Inflow Region

Given the above justifications for employing steric sea leveling methods, I now examine particular topographies of the sea surface in the inflow region using data acquired during JMA70 (Fig. 2). In this analysis, I choose a reference level of 400 db as established in Section IV-D above.

During JMA70, each of the sections A-F was occupied four times during the experiment at roughly 1-week intervals, thus giving four

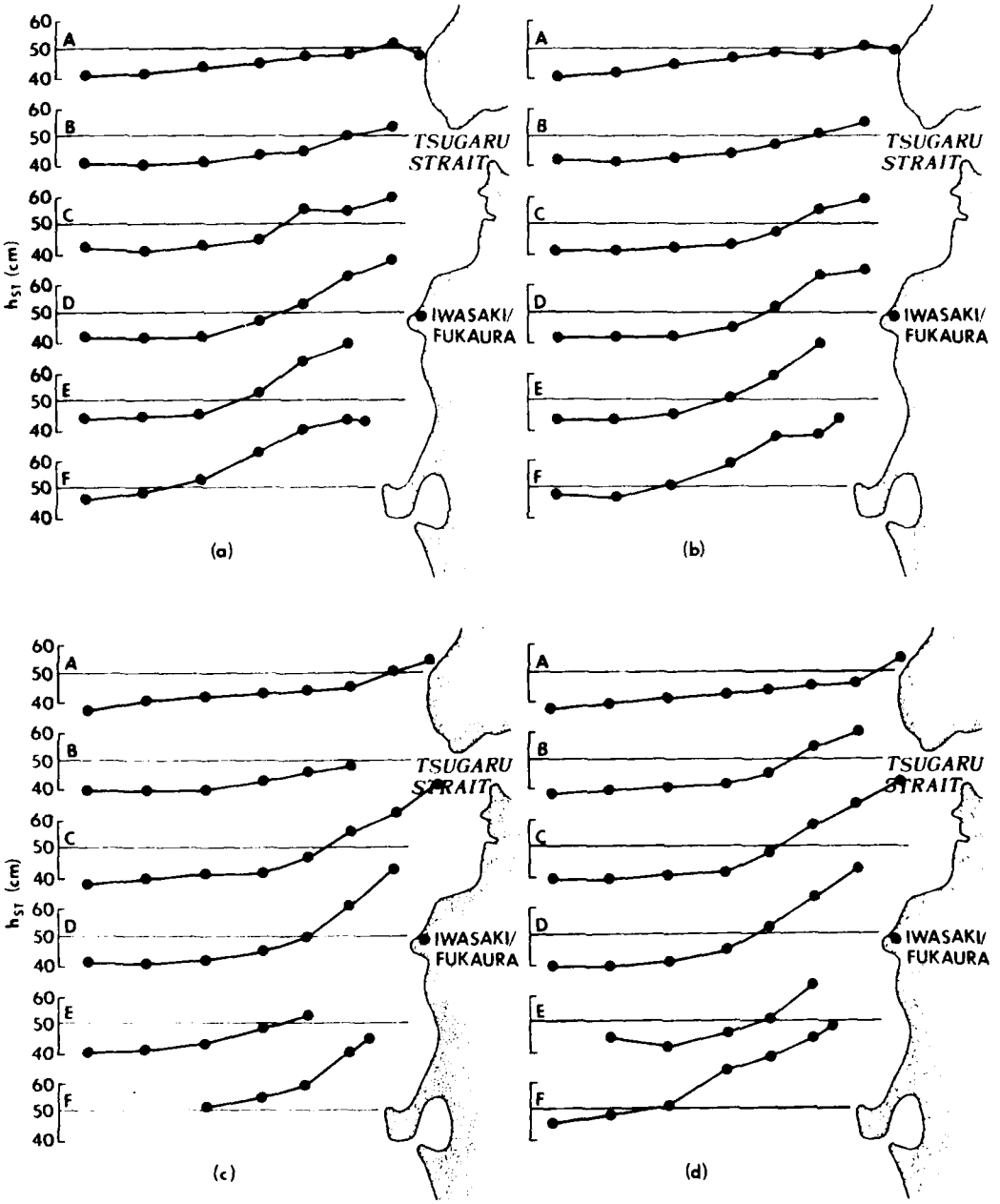

Figure 10. Steric height variations in inflow region of Tsugaru Strait during JMA70 (0/400 db); (a) Run I, (b) Run II, (c), Run III, (d) Run IV.

quasi-synoptic views of the inflow region. These runs are designated as follows:

Run	Dates
I	October 14-17
II	October 21-22
III	October 28-29
IV	November 2-3

Steric height variations across each section and for each run are plotted in Figure 10a-d. Note, first, that the offshore stations (longitude 138°00'-138°20') show very little variation in steric heights throughout the experiment. These stations represent ambient Sea of Japan conditions, and in this analysis represent the "far-field" limit. The Tsushima Current is generally confined to a region inshore of latitude 138°30' east, in which the setup induced across the southern sections (C-F) reaches 30 cm and more. The inshore stations show a steady decrease in setup, especially in the vicinity of the strait (at the latitude of section B). Note, for example, that the drop in steric height between stations C8 and A8 in Runs III-IV is about 18 cm, equivalent to a sea surface slope of about 2.4×10^{-6}.

For a more quantitative analysis of the steric height variations, I isolate sections A and D for attention. Section A is the northernmost, and it will provide data to measure the northern volume transport which bypasses the strait. Section D is the southernmost section for which no data are missing, and it is sufficiently far from the strait to provide accurate information on Tsushima Current inflow. Furthermore, the close proximity of station D7 to Iwasaki/Fukaura will permit a comparison to be made between steric sea level values and sea level data acquired at coastal station tied to Iwasaka/Fukaura by land (geodetic) leveling.

Sections D and A will be used to construct a transport budget for the Tsushima Current; that is, the northern flow through D, minus the northern flow through A, should give a measure of transport into the strait. I restrict the calculations to Stations D2 and A2 on the western boundary; transport across the north-south section through these stations is negligible, and the steric heights at these stations differ by a maximum of 0.6 cm.

Steric heights for stations D2, D7, A2, and A8 are given in Table 1, and differences of steric heights are shown in Table 2 for key station pairs. The hydrographic measurements from which these values are derived are subject to a standard error in thermosteric anomaly of about 0.2×10^{-5} ml/g at each depth. Each station typically comprised measurements at 14 levels, giving a standard error at any station of about 0.7×10^{-5} ml/g. Over a depth of 400 m, the standard error in steric sea level should therefore be less than 0.3 cm; for differences between stations, the standard error should be about 0.4 cm.

The cross-stream steric height difference Δh_D = D7-D2 (Tsushima Current setup) varies from 23.2 to 33.2 cm, with a mean value of 29.2 cm. North of the strait, however, the cross-stream height difference Δh_A =

Table I

Steric Heights (cm) Referenced to 400 db

Station	I	II	III	IV
D7	68.2	64.3	73.8	72.7
D2	41.1	41.1	40.6	39.5
A8	49.1	49.3	55.1	55.6
A2	41.7	41.7	41.0	39.1

A8-A2 averages 11.4 cm, a reduction of 17.8 cm. Note that because the offshore slope (A2-D2) varies so little, this reduction closely matches the inshore drop in steric height (D7-A8), which averages 17.4 cm.

Sturges (1968, 1974) examined the northward variation of cross-stream height difference Δh in the Gulf Stream and found that the northward decrease in coastal sea level was attributable to the beta effect. In his analysis, Sturges differentiated equation (9) with respect to y to obtain

$$\frac{\partial \Delta h}{\partial y} = \frac{f}{g} \frac{\partial \langle v \rangle X}{\partial y} + \frac{\langle v \rangle X}{g} \frac{\partial f}{\partial y} \qquad (10)$$

If the offshore edge of the current is level, the left-hand side is the meridional slope in sea level along the coast. The first term on the right represents net gain or loss of surface transport. Based on direct measurements of average surface transport in the Gulf Stream, Sturges concluded that this term was negligible.

If one applies (10) to the inflow region of the Tsugaru Strait, the results are dramatically different. Sections A and D are separated by 1° of latitude, and so the slope term in (10) is about -17.8 cm/deg. To evaluate the beta effect term, I use the value $\langle v \rangle X \sim 3 \times 10^8$ cm^2/sec, obtained from the analysis of stations CM1-CM5; the change in f between D and A is about 2×10^{-6}; so the magnitude of the beta term is about 0.6 cm/deg, a negligible value. This means that the slope term (sign negative) should be almost totally balanced by a net loss of surface transport, i.e., flow into the strait.

This meridional drop in sea level during JMA70 can be compared to results of land leveling. In 1972 the tide gauge at Oshoro (see Fig. 1) was tied to a first-order leveling network that included Iwasaki/Fukaura. I have analyzed monthly mean tides for these two locations for the period 1972-1976 and found that the mean drop in sea level in October between Iwasaki/Fukaura and Oshoro was 16.8 cm. Oshoro is at latitude 43°12.4'N, so the beta term is about 1-2 cm, still an order of magnitude less than the slope term. The results of steric leveling and land leveling thus appear to agree quite favorably.

Table 2
Steric Sea Level Differences (cm)

Stations	Run I	Run II	Run III	Run IV	Comment
D7-D2	27.1	23.2	33.2	33.2	Δh_D
A8-A2	7.4	7.6	14.1	16.5	Δh_A
D7-A8	19.1	15.0	18.7	17.1	Inshore sea level change
D2-A2	-0.6	-0.6	-0.4	+0.4	Offshore sea level change

G. Volume Transport into the Tsugaru Strait

Table 3 presents the results of a transport budget calculation in which transport into the Tsugaru Strait is computed for each run of JMA70. In this calculation, the northward volume transport through D2-D7, less the volume transport through A2-A8, is equal to the transport into the strait. As previously noted, transport through the western boundary is negligible.

If we compare meridional drop in sea level (D7-A8) with strait intlux, we find a linear relationship with a high correlation coefficient:

$$T(Sv) = 7.85 \times 10^{-2}\ \Delta h(cm) + 0.30 \quad (r = 0.98)$$

(Note the small residual for $\Delta h = 0$). From this relation, we conclude that transport into the strait is associated with a "relaxation" of setup induced by the Tsushima Current in the vicinity of the Tsugaru Strait. If so, then the ultimate forcing factor of flow into the strait is the forcing of the Tsushima Current; because the Tsushima Current is part of the Kuroshio system, this forcing must be of a much larger scale than that considered in this thesis.

Apart from this large-scale forcing, however, we must consider other local factors that can affect transport into the strait.

Table 3
Section Geostrophic Transports (Sv)

	Run I	Run II	Run III	Run IV
Section D	2.6	2.4	3.6	3.6
Section A	0.8	0.9	1.8	2.0
Into Strait (D-A)	1.8	1.5	1.8	1.6

1. Low-pressure systems in the Sea of Japan. Hata (1975) analyzed volume transport in the Tsugaru Strait region for the years 1933-1969 and found that low pressure systems passing through the Sea of Japan brought about intensification of the Tsushima Current and increased volume transport through the Tsugaru Strait. Hamano (1977) noted that during JMA70 a low-pressure system passing through the inflow region on October 25-26 was accompanied by an increase in northward transport of the Tsushima Current. (This storm occurred between Runs II and III; see Table 3.)

While the importance of such effects is unequivocal on a time scale on the order of 1-10 days, low pressure systems are not a permanent feature of the Sea of Japan, and cannot be responsible for the steady exchange between the Sea of Japan and the North Pacific.

2. Sea of Japan - North Pacific sea level difference. It has been noted by several authors (e.g., Iida, 1972) that long-term tide gauge records show that monthly mean sea level at Iwasaki/Fukaura is on the average 20 cm higher than at Hachinohe, on the North Pacific coast (see Fig. 1). In Figure 11 the monthly difference for the period 1969-1976 (following a first-order leveling in 1969) is displayed. Although this sea level difference appears to suggest a "sink" flow from the Sea of Japan to the North Pacific, there are two reasons why I think this is not the case.

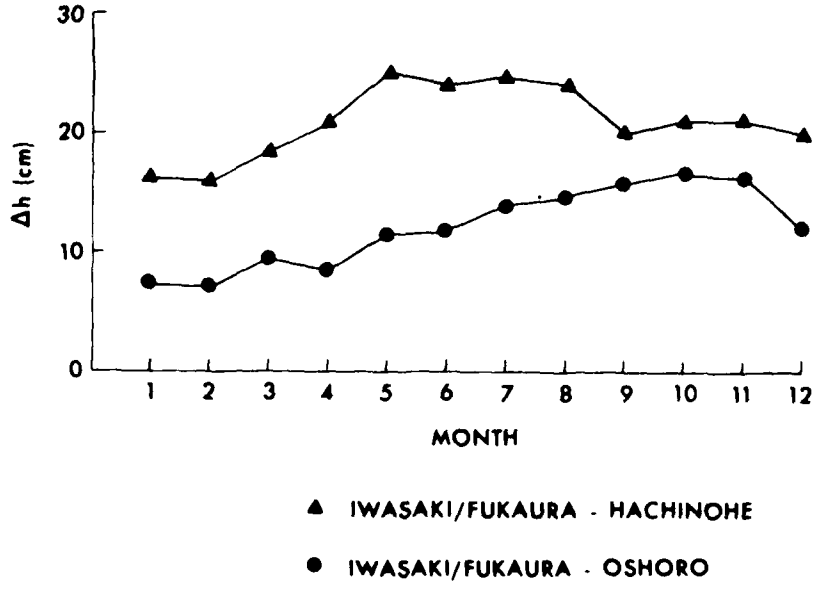

Figure 11. Seasonal sea level difference based on monthly mean tide gauge records for the period 1972-1976. Above: Iwasaki/Fukaura minus Hachinohe. Below: Iwasaki/Fukaura minus Oshoro. See Figure 1 for locations.

First, the annual cycle of the mean sea level difference looks wrong. I have presented evidence that strongly supports the correlation between meridional drop across the Tsugaru Strait and transport into the strait, and the seasonal nature of this correlation can be well approximated by a plot of monthly mean sea level difference between Iwasaki/Fukaura and Oshoro (also plotted in Fig. 11). Note that this seasonal variation is consistent with the findings of Hata (1962) and others (winter transport minimum, fall maximum), while the I/F-Hachinohe sea level difference shows a spring maximum with a decline in value in the fall. (Atmospheric pressure differences for each station pair are typically 1 cm or less.)

Second, steric leveling results show that in the far-field region in the Sea of Japan (away from the influence of the Tsushima Current), sea level appears to be lower than at Hachinohe. In October 1970, for example, the mean sea level difference between Iwasaki/Fukaura and Hachinohe was 21.4 cm, while the average steric difference across D2-D7 was 29.2 cm for Runs I-IV of JMA70. Further evidence of this is provided in Figure 12, in which calculations have been made of steric differences between offshore stations and those inshore stations on which Figure 9 was based. A comparison of Figures 9 and 12 shows that, except for May (one value of steric heights), the inshore-offshore difference is greater than the I/F-H difference by 2-5 cm. Finally, the average meridional drop in sea level during JMA70 was 17.4 cm, which is close to the value of the October I/F-H sea level difference. The evidence cited here leads to the logical conclusion that the Sea of Japan/North Pacific sea level difference is principally generated by the Tsushima Current, and that the diversion into the Tsugaru Strait occurs because the increased sea level in the Sea of Japan cannot be maintained when the coastline vanishes at the entrance to the strait.

It can be argued that because sea level at Hachinohe is influenced by the Tsugaru Warm Current it may not be representative of the "far-field" sea level in the North Pacific. The complex nature of the Tsugaru Warm Current (see Chapter VI) does not lend itself to such a simple treatment as was employed for Iwasaki and Section D. Some evidence for far-field behavior, however, can be obtained by steric sea leveling through the Tsugaru Strait. Lisitzin (1965) has pointed out that steric leveling between adjoining basins must be limited to that depth at which the basins have free communication; if the basins are connected by a shallow strait, then the sill depth is the maximum reference surface. For the Tsugaru Strait, a 125-db surface is a reasonable approximation. During JMA70, all stations on both sides of the strait were occupied during the period October 30-November 3. Assuming that minimum steric heights are most representative of far-field conditions, I found that the minimum height referenced to 125 db in the Sea of Japan was about 18 cm, while on the North Pacific side the value was about 26 cm. Sea level in the Sea of Japan again appears lower than that of the adjacent North Pacific. Lisitzin (1965) found that, in general, marginal seas have lower sea level than their adjacent oceans, and these results are consistent with her findings.

A rough picture of variation in sea level in this region can be provided using the October 30-November 3 data. If sea level in the far-

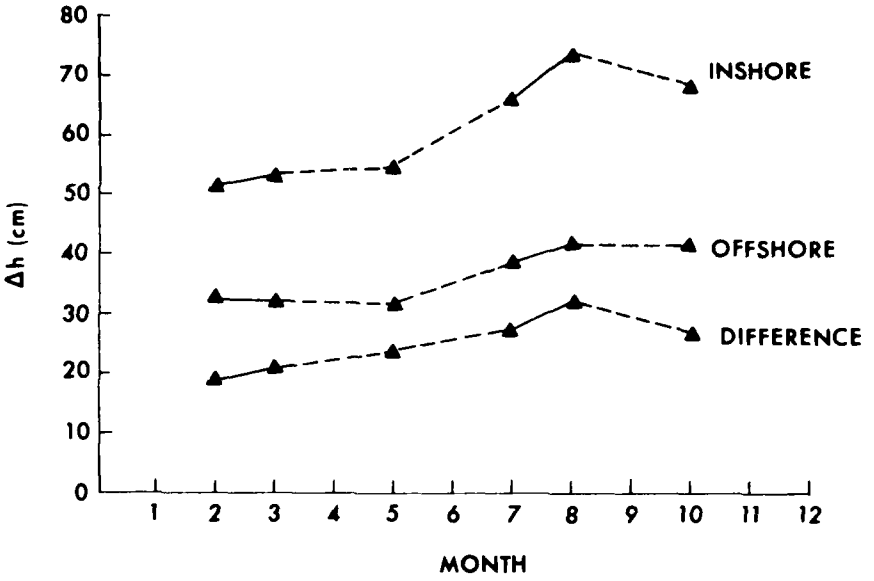

Figure 12. Seasonal steric heights calculated from hydrographic station pairs, 1956-1976, near latitude 40°40'N. Inshore: stations near longitude 139°45'E. Offshore: stations near longitude 138°E. The offshore variation represents steric variation induced by seasonal heating and cooling. The difference between inshore and offshore steric heights represents steric variation induced by advection (i.e., seasonal variation of northward Tsushima Current transport).

field Sea of Japan is 18 cm (0/125 db), and it gains 33 cm proceeding across the Tsushima Current (D2-D7) and then loses 17 cm transiting the strait (D7-A8), then sea level at the western entrance to the Tsugaru Strait would be 34 cm, or about 8 cm higher than in the North Pacific (26 cm). This value is encouragingly close to the value of 6.5 cm that will be cited in Chapter V as a representative drop in sea level within the Tsugaru Strait.

CHAPTER V

THE TSUGARU STRAIT

A. Introduction

The volume transport budget presented in the previous chapter showed that transport into the Tsugaru Strait during JMA70 varied between 1.5 Sv and 1.8 Sv. Hata (1962) performed a similar calculation for sections on latitudes 41°N and 42°N during the years 1947-59 and found that transport into the strait varied from 1 Sv to 4 Sv. This is an extremely large net transport for a strait that at its narrowest point is barely 20 km wide, and the principal question to be addressed in this chapter is: What is the effect of such large net transport on the flow regime within the strait?

B. Physical Geography of the Tsugaru Strait

The Tsugaru Strait lies between the islands of Honshu and Hokkaido and has a general orientation of southwest to northeast (Fig. 13). The strait is approximately 20 km wide at both its western narrows (Tappi Saki to Shirakami Saki) and eastern narrows (Oma Saki to Toi). In the central part, the strait widens to a breadth of about 50 km between Hakodate and the entrance to Mutsu Wan. Mutsu Wan has a surface area on the order of 600 km^2 and a mean tide range of 1 m, giving it a tidal prism of about 6×10^8 m^3, or less than the volume of water that passes through the Tsugaru Strait in 10 minutes. The presence of Mutsu Wan will therefore be neglected in the sections that follow.

The strait has a western sill of approximately 125-m depth, but has no identifiable sill at the eastern end. Beyond the western narrows, the principal channel gradually deepens toward the northeast; along the line Oma Saki-Toi, the maximum depth is about 250 m. However, the cross-sectional areas of the channel at the western and the eastern narrows are quite similar, about 2.2 km^2 versus 2.5 km^2; mean depths across these sections are roughly 115 m in the west versus 130 m in the east.

C. Currents

1. Mean currents. The surface flow field within the Tsugaru Strait has been studied by Suda et al. (1932), Hikosaka (1953), Hata et al. (1964), and the Japan Maritime Safety Agency (Science and Technology Agency, 1979), and there is general agreement on the principal features (Fig. 14). The surface current displays a high-speed core about 20 km wide in which flow is from west to east at speeds typi-

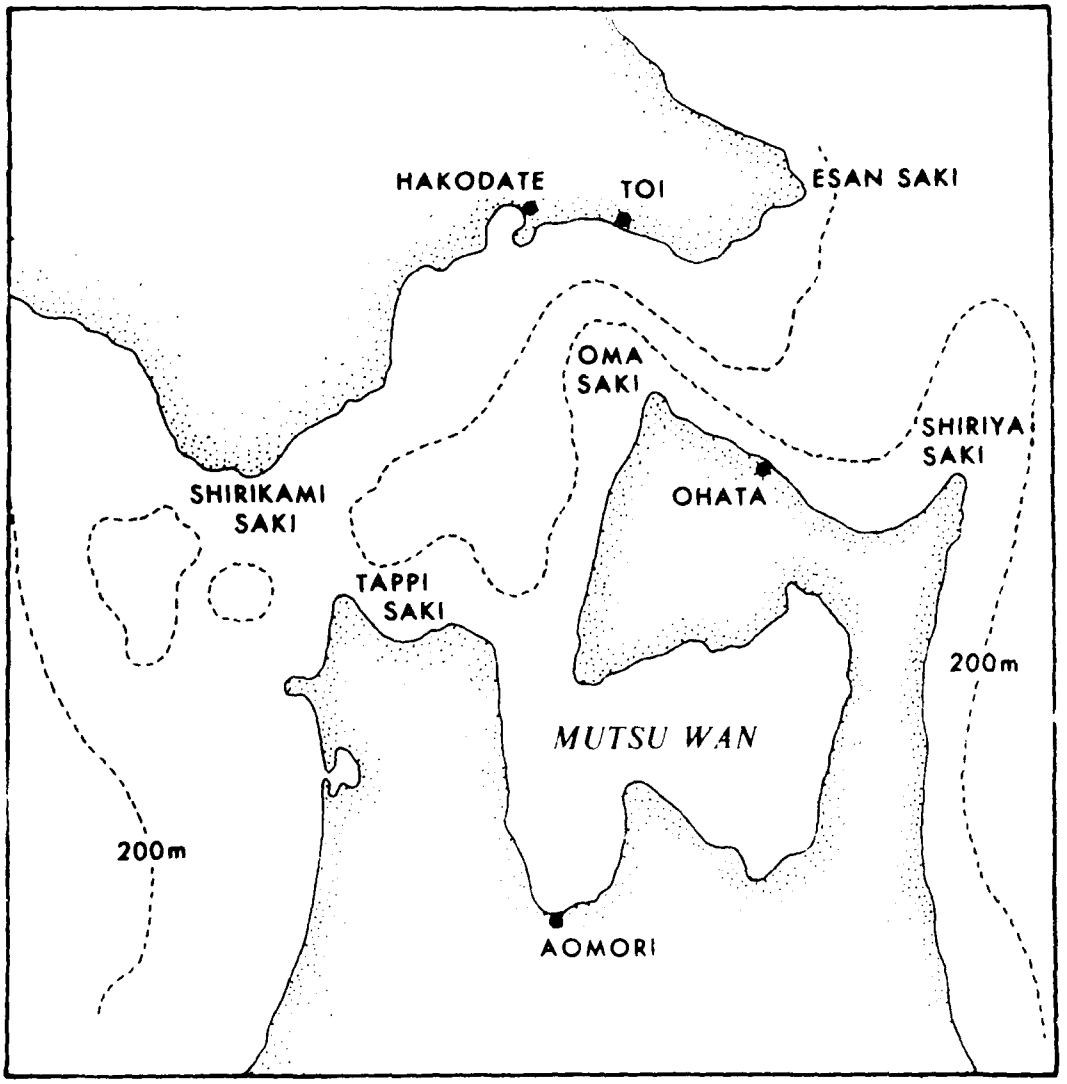

Figure 13. Map of Tsugaru Strait with 200-m isobath lines.

cally of 2 knots. Along both sides of the core, semi-permanent sidewall eddies are seen in regions where the channel broadens--cyclonic eddies along the northern boundary and anticyclonic eddies in the south.

Suda et al. (1932) performed a series of observations on subsurface currents at various locations within the strait and found that a lower layer return flow typical of most straits is largely absent. Near the western narrows, flow is typically from west to east, from the surface to the bottom. A weak flow is found only at depths on the order of 200 m, and is generally found toward the eastern narrows where the main channel deepens.

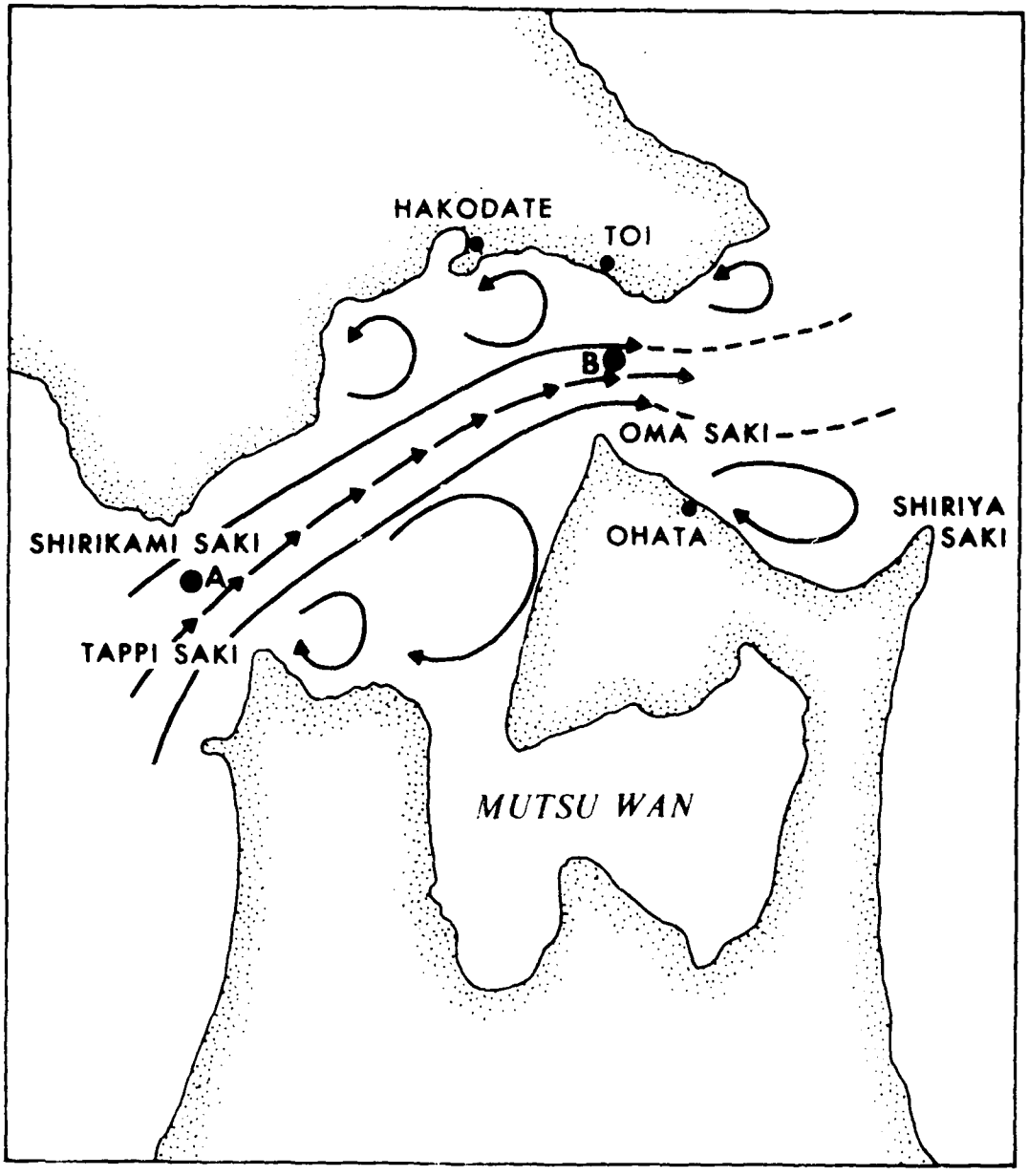

Figure 14. Typical surface flow pattern within the Tsugaru Strait (after Hata et al., 1964). A and B refer to locations of surface current observations of Suda et al. (1932), referred to in Section V-D.

2. Tidal currents. Ogura (1933) made an extensive study of the tides in the Tsugaru Strait and found that they are of the mixed type, with a ratio $(K_1 + O_1)/(M_2 + S_2) = 0.8$. The M_2 tide arrives nearly simultaneously at both ends of the strait, but the spring range decreases sharply from about 90 cm at the east end to about 15 cm in the west. The diurnal tide, on the other hand, moves very slowly through the strait from east to west; the range of the diurnal tide also varies sharply,

from 80 cm at the east end to about 20 cm in the west.

Tidal currents, however, are chiefly diurnal. The results of measurements performed during JMSA75 show a diurnal amplitude of about 2 knots, with tidal currents slightly stronger near the eastern narrows than in the west. Even though the tidal currents are strong, the influx of the Tsushima Current water is so overwhelming that reversals of current in the strait are very infrequent (Fig. 15).

D. Momentum Balance in the Strait

In this section, I wish to assess the principal dynamic balance of flow in the Tsugaru Strait. In the following treatment, I will therefore restrict my attention to the current core (order of 20 km wide) that exists between the western and the eastern narrows, and I will neglect the sidewall eddies.

In the steady state, the core shows little lateral spreading along the length of the strait, and so to a reasonable approximation I can neglect lateral motion. In a coordinate system in which x is positive downstream, y is positive to the left, and z is positive downward, the cross-stream momentum balance simply reduces to a geostrophic balance:

$$0 = \frac{-1}{\rho}\frac{\partial p}{\partial y} - fu \ . \tag{11}$$

The longitudinal momentum equation, excluding lateral motion, is

$$\frac{\partial u}{\partial t} + \frac{u\partial u}{\partial x} = \frac{-1}{\rho}\frac{\partial p}{\partial x} + Ax\frac{\partial^2 u}{\partial x^2} Ay\frac{\partial^2 u}{\partial y^2} + A_z\frac{\partial^2 u}{\partial z^2} \tag{12}$$

I wish to consider steady-state conditions, and so I will first average equation (12) over a tidal cycle. The instantaneous velocity u(x,t) can be written as

$$u(x,t) = U(x) + C(x)\cos\frac{2\pi}{T}t \tag{13}$$

where U(x) is the mean velocity of the current as a function of position along the channel, C(x) is the amplitude of the tide, and T is the period of the tide (~24 hours). Substituting (13) into (12) and performing the necessary integration yields

$$u\frac{\partial u}{\partial x} + 1/2C\frac{\partial C}{\partial x} = -\frac{1}{\rho}\frac{\partial p}{\partial x} + Ax\frac{\partial^2 u}{\partial x^2} + Ay\frac{\partial^2 u}{\partial y^2} + Az\frac{\partial^2 u}{\partial z^2} \tag{14}$$

where u is now a time-averaged quantity.

There does not exist a complete data set for the Tsugaru Strait that would permit simultaneous estimates of the terms of equation (14) to be made. Therefore, I will cite experimental data that will give us reasonable orders of magnitudes of the contributions of each term.

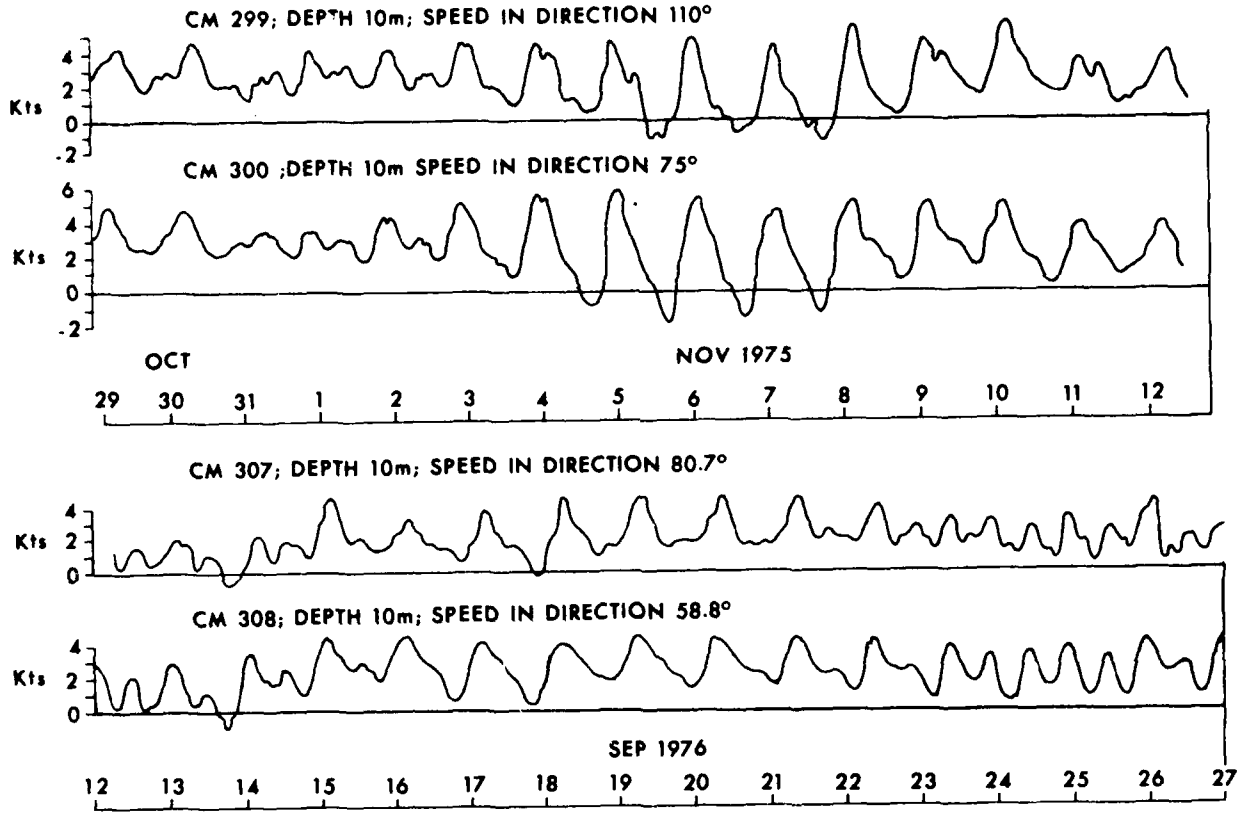

Figure 15. Near-surface currents in the Tsugaru Strait during JNSA75 (see Fig. 4 for locations). Currents shown are along principal axes of flow.

First, the barotropic part of the pressure gradient term, $g\,\partial\zeta/\partial x$, can be estimated from tide measurements made during JMSA75. Temporary stations at Tappi Saki, Yoshioka, Ohata, and Toi were occupied during January and July 1977 (see Fig. 14). The mean longitudinal drop in sea level was 6.5 cm during both periods; as the station pairs were separated by a longitudinal distance of 70 km, the order of magnitude of the pressure gradient term to a good approximation is 10^{-3} (cgs).

Suda et al. (1932) obtained surface current measurements at stations A and B (Fig. 14) at the western and the eastern narrows in 1924, 1929, and 1931. They found that the downstream velocity increased by about 10 cm/sec between A and B, and that the sum of tidal components $K_1 + O_1$ was less than 10 cm/sec higher at Station B than at Station A. Therefore, we can estimate the longitudinal gradients $\partial u/\partial x$ and $\partial C/\partial x$ to be 10 cm/sec/70 km $\simeq 10^{-6}$ (cgs). For characteristic velocities of u = C = 100 cm/sec, the nonlinear terms on the left-hand side of (14) both have magnitudes of about 10^{-4}.

The longitudinal Ekman term $Ax\ \partial^2 u/\partial x^2$ can be estimated using $Ax = 10^8$, $\partial u/\partial x = 10^{-6}$, and $X = 7 \times 10^6$, giving an order of magnitude of 10^{-5}.

Sufficient field data do not exist to explicitly evaluate the lateral Ekman term $A_y\ \partial^2 u/\partial y^2$, but a reasonable order-of-magnitude estimate can be made. Velocity differentials across the core appear to be small, on the order of 10 cm/sec, while across the sidewall eddies the velocity can change by an order of 100 cm/sec. Taking the width of the core to be 20 km and that of the sidewall eddies to be 10-15 km, and taking $A_y = 10^8$ cm^2/sec, the lateral Ekman term is on the order of 10^{-4} in the core and 10^{-3} in the sidewall eddies.

The vertical Ekman term cannot be neglected. Using order-of-magnitude estimates of $A_z = 10^3$, $u = 10^2$, and $z = 10^4$ (cgs), the magnitude of this term is on the order of 10^{-3}.

Summarizing, the estimates of the terms in (14) are as follows:

$$10^{-4} + 10^{-4} = 10^{-3} + 10^{-5} + \left\{\begin{matrix} 10^{-4} \text{ (core)} \\ 10^{-3} \text{ (eddies)} \end{matrix}\right\} + 10^{-3} \,. \qquad (15)$$

The principal balance within the core current thus appears to be between the pressure gradient term and the vertical Ekman term, an "antitryptic balance" in Defant's (1961) terminology. Within the sidewall eddies, the lateral Ekman term appears to be not negligible.

Previous investigators (e.g., Miyazaki, 1952; Science and Technology Agency, 1972) have attempted to model the flow through the strait as a balance between the nonlinear term $u\,\partial u/\partial x$ and barotropic pressure gradient $g\,\partial\zeta/\partial x$. In these attempts, the longitudinal drop in sea level was taken to be the difference in mean sea level between Iwasaki/Fukaura and Hachinohe, about 20 cm. As we have seen in Chapter IV, this is a poor estimate of sea level drop in the strait because most of the 20-cm difference is lost in the turning process. Not surprisingly, this "Bernoulli balance" gives poor results. Previous investigators con-

cluded that friction must be important in the strait, which agrees with the present analysis.

Even with the more accurate estimate of a 6.5-cm longitudinal sea level drop, the Bernoulli balance still gives poor results. Such a balance can be expressed as

$$\frac{U^2}{2} + g\zeta = \frac{U_o^2}{2} + g\zeta_o \tag{16}$$

where u_o, ζ_o are values of velocity and mean sea level at the head of the strait. With U_o = 100 cm/sec and $\Delta\zeta$ = 6.5 cm, equation (16) predicts an acceleration of the current by about 50 cm/sec, or five times that observed by Suda et al. (1932). While not conclusively proving that the nonlinear term $u\,\partial u/\partial x$ is negligible, such a calculation shows that the antitryptic balance appears to be more appropriate.

E. A Simplified Model of Strait Flow

I wish now to test the results of the previous section in a simplified model of flow in the Tsugaru Strait. Given the geography of the strait and the nature of the core current, it seems appropriate to consider a rectangular channel 20 km wide and 125 m deep. The momentum equation employed is, again,

$$0 = -\frac{1}{\rho}\frac{\partial p}{\partial x} + A_z \frac{\partial^2 u}{\partial z^2} \quad . \tag{17}$$

Noting that atmospheric pressure gradients on the scale of the strait will again be negligible, and again allowing for vertical variations in density, we substitute (6) into (17) and rearrange to yield

$$\frac{d^2u}{dz^2} = -\frac{g\alpha}{A} + \frac{g}{\rho A}\int_o^z \frac{\partial \rho}{\partial x}\,dz \tag{18}$$

where $u = u(z)$ only and $\alpha = \partial\zeta/\partial x$. The subscript of A has been dropped for brevity.

At the surface, I allow a wind stress

$$\tau = \rho_a C_D |w| w = -\rho_s A \frac{du}{dz}$$

where $\rho C_D = 1.44 \times 10^{-6}$ (cgs), ρ_a = density of air, w = wind speed, and ρ_s is the surface density of the water.

At the bottom, I impose a quadratic friction law

$$f_b = k\,\rho_b |u_b|\, u_b = -\rho_b A \frac{du}{dz} \qquad z = h$$

where ρ_b = density of water at the bottom and u_b = bottom velocity. Note that because the bottom velocity does not reverse in a tidal cycle, we can write

$$f_b = k\,\rho_b\,u_b^2 \tag{19}$$

At the bottom, the velocity is composed of a mean and a tidal component:

$$u_b = \bar{u}_b + C_b \cos\frac{2\pi}{T}\,t$$

so, upon time averaging, the bottom friction becomes

$$f_b = k\,\rho_b\,(U_b^2 + 1/2\,C_b^2) \tag{20}$$

where U_b is now the mean velocity.

With these boundary conditions, the solution for the vertical velocity profile is:

$$u = \frac{g\alpha}{2A}(h^2 - z^2) - \frac{g}{\rho A}\left(\int_o^h\int_o^z\int_o^{z'}\frac{\partial\rho}{\partial x}\,dz''\,dz' - \int_o^z\int_o^{z'}\int_o^{z''}\frac{\partial\rho}{\partial x}\right.$$

$$\left.dz'''\,dz''\,dz'\right) + \frac{\tau}{\rho_s A}(h - z) + D \tag{21}$$

where

$$D = \frac{g\alpha h}{k} - \frac{g}{k\rho}\int_o^h\int_o^z\frac{\partial\rho}{\partial x}\,dz'\,dz + \frac{\tau}{\rho_s k} - \frac{1}{2}C_b^2 \tag{22}$$

Note that at $z = h$, $u = D$ = bottom velocity u_b.

In order to gain some insight into the physical meaning of (21), I will consider some simplified cases.

Case 1: $\tau = 0$, $\partial\rho/\partial x = 0$, $C_b = 0$

Here we can see the basic result of a barotropic pressure gradient acting against friction. If we insert the value of $A = 10^3$ cm^2/sec into (21) and use a normal bottom friction factor $k = 2.5 \times 10^{-3}$, we find that $u\ (z = 0) = 147$ cm/sec, which is well within a factor of 2 of measured mean surface currents. The bottom velocity is calculated to be 70 cm/sec. We can integrate (21) with depth to find the transport per unit channel width:

$$r = \frac{g\alpha}{6A}h^3 + \left(\frac{g\,\alpha\,h^3}{k}\right)^{1/2} \tag{23}$$

For $A = 10^3$, $k = 2.5 \times 10^{-3}$, the value of r is:

$$r = 3.19 \times 10^5 + 8.75 \times 10^5 = 1.2 \times 10^6 \text{ cm}^2/\text{sec}$$

and for a channel of width 20 km, the total volume transport is about 2.4 Sv, again a value in normal bounds.

Defant (1961) has suggested that the friction factor k in straits appears to be much higher than normal, on the order of 10^{-2} or even 10^{-1}. He also used lower values of A in his study of the Bosporus, between 300 and 500 cm^2/sec. In Table 4, I tabulate the results of using various combinations of A and k in equations (21) and (23). Note that for A = 500, the surface velocities are about 4 knots, which is much too high. For A = 1,000, both values of k give results within reason, but it is clear that this calculation is sensitive to a choice of friction factor.

Case II: $\partial\rho/\partial x = 0$, $C_b = 0$, $\tau \neq 0$.

As indicated in Chapter III, a wind stress of +1 dyne/cm^2 is a reasonable figure to use for this sensitivity analysis. For $A = 10^{-3}$, $k = 2.5 \times 10^{-3}$, $\tau = 1$ (cgs), equation (21) yields $u(z = 0) = 159$ cm/sec; i.e., a wind stress of 1 dyne/cm^2 increases the surface velocity by only about 10 cm/sec. The transport per unit width is now

$$r = \frac{g\alpha}{6A} h^3 + \left(\frac{g \alpha h^3}{k}\right)^{1/2} + \frac{\tau h^2}{2\rho A}$$

which for our channel gives a transport of T ~ 2.5 Sv, an increase of only 0.1 Sv from the Case I calculation. It therefore appears that for winds less than 5 m/sec the contribution of wind stress to the calculation can be neglected.

Table 4
Calculated Surface Currents and Sectional Transports for Combinations of A and k Using Eq. 21 with $\tau = 0$, $\partial\rho/\partial x = 0$

	A(cm^2/sec)	
k	10^3	5×10^2
2.5×10^{-3}	U_s = 147 cm/sec T = 2.4 Sv	U_s = 223 cm/sec T = 3.0 Sv
1.0×10^{-2}	U_s = 110 cm/sec T = 1.5 Sv	U_s = 190 cm/sec T = 2.2 Sv

Case III: $\tau = 0$, $\partial\rho/\partial x = 0$, $C_b \neq 0$

An examination was made of unpublished data from a 4-week mid-summer deployment of current meters in the western entrance of the Tsugaru Strait (data courtesy of R. W. Stewart). The near-surface data show an easterly current of slightly more than 100 cm/sec, modulated by a diurnal tidal current of roughly 100 cm/sec amplitude. Five metres above the bottom, a mean current of slightly less than 50 cm/sec was observed (also easterly), modulated by a tidal component of about 20 cm/sec amplitude.

If we use the values $C_b = 20$ cm/sec, $k = 2.5 \times 10^{-3}$ in equation (22), we see that inclusion of the effect of bottom tidal motion gives a value of U_b (mean) of 68.5 cm/sec versus 70 cm/sec from the previous calculation. If $k = 0.01$, the reduction in U_b is still less than 10%. In the mean, therefore, we can neglect the effect of bottom tidal motion.

Case IV: $\tau = 0$, $C_b = 0$, $\partial\rho/\partial x \neq 0$

The Case I calculation gave a bottom velocity of $U_b \sim 70$ cm/sec, but the long-term mooring data give a mean velocity of $U_b \sim 50$ cm/sec. This is a difference too large to ignore, and we look to the longitudinal baroclinic pressure gradient to see if this difference can be resolved.

Let us first consider the situation where $\partial\rho/\partial x$ is constant with depth, analogous to a well-mixed estuary. In that case, the second term of equation (21) is

$$-\frac{g}{6\rho A}\frac{\partial\rho}{\partial x}(h^3 - z^3)$$

and the bottom velocity is

$$D = \left(\frac{g\alpha h}{k} - \frac{g}{2k\rho}\frac{\partial\rho}{\partial x}h^2\right)^{1/2}.$$

A simple calculation shows that a reduction of bottom velocity from 70 cm/sec to 50 cm/sec can be achieved (using $k = 2.5 \times 10^{-3}$) if $\partial\rho/\partial x \sim 7.8 \times 10^{-11}$ (cgs), which corresponds to a density increase of only about 0.5 σ_T units in 70 km of strait length. With this value of $\partial\rho/\partial x$, the mean surface current would be reduced to 102 cm/sec, compared to the Case I calculation of 147 cm/sec, an appreciable effect.

For a test calculation, I employ STD data from stations occupied by the USNS SILAS BENT in November 1975 (Fig. 16). Stations 30, 22, and 21 indicate a positive $\partial\rho/\partial x$ along the path of the Tsushima Current into the Tsugaru Strait. Stations 22 and 21 display intense mixing within the strait, with a reversal in sign of $\partial\rho/\rho x$ at about 75 m. The maximum density gradient between stations 22 and 21 is nearly 16×10^{-11} (cgs) at 45-m depth, which from the considerations in the previous paragraph we know is a significant gradient.

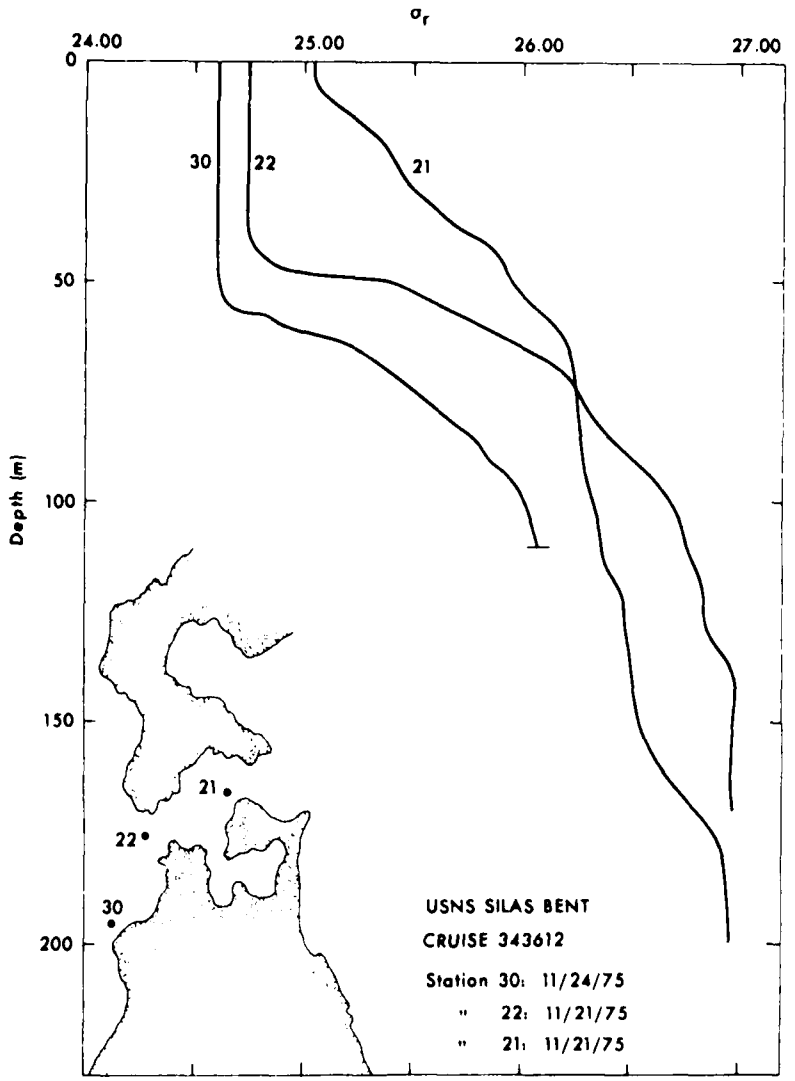

Figure 16. STD profiles obtained during cruise of USNS SILAS BENT, November 1975.

Limiting the calculation to a depth of 125 m, I calculated the vertical profile of the longitudinal baroclinic pressure gradient $-g/\rho_o \int_z^0 \partial\rho/\partial x \, dz$. The maximum value of this quantity is about -5.8×10^{-4} at 75 m, which is nearly 60% of the value of the barotropic pressure gradient ($\sim+10^{-3}$). Performing the higher integrations of equation (21), I find that for $A = 10^3$, $k = 2.5 \times 10^{-3}$ the bottom velocity is reduced to 54 cm/sec and the surface velocity to 104 cm/sec, values that closely approximate those measured by the long-term current meter moorings. Total volume transport is reduced to about 2.1 Sv.

In conclusion, existing data sets do not permit a simultaneous calculation to be made of each significant term in the longitudinal

momentum balance. Nevertheless, there is sufficient information on which a reliable estimate can be made of the principal momentum balance in the Tsugaru Strait. The analysis above shows that the longitudinal barotropic gradient is mainly balanced by the longitudinal baroclinic pressure gradient and friction. At low to moderate speeds, wind stress appears to be of second-order importance, as does the nonlinear acceleration $u\,\partial u/\partial x$. The longitudinal Ekman term is negligible; the lateral Ekman term is probably appreciable in the region of the sidewall eddies, but is probably not significant within the core itself.

F. A Hansen-Rattray Diagram for Sea Straits

In this the final section of this chapter, I would like to attempt to relate the characteristics of the Tsugaru Strait to the characteristics of other sea straits. If successful, we might be better able to assess the dynamic similarities and differences of straits, thereby improving our ability to judge the applicability of insights gained in one area to other straits in quite different environmental settings.

Hansen and Rattray (1966) have devised a classification scheme for estuaries that uses simple parameters to describe circulation and stratification. In the Hansen-Rattray diagram shown in Figure 17, the ordinate is the ratio of the surface-to-bottom salinity difference δS to the mean cross-sectional salinity S_o; the abscissa is the ratio of net surface current velocity U_s to the mean cross-sectional velocity U_f. In a Type 1 estuary, the net flow is seaward at all depths and the up-estuary salt flux is entirely by diffusion. Type 1a is an archetypal well-mixed estuary, while in Type 1b there exists significant stratification. Type 2 corresponds to a partially mixed estuary; flow reverses with depth, and both advection and diffusion are important in the salt flux. In Type 3 estuaries, the salt flux is almost totally by advection. In Type 3b, the lower layer is so deep that circulation does not extend to the bottom; fjords are usually Type 3b. Type 4 is the salt-wedge estuary, in which there is still greater stratification; from Type 4 to Type 3, the flow varies from a thick upper layer flowing over a thin lower layer to a thin surface layer flowing over a deep lower layer. The upper boundary of the diagram represents fresh-water outflow over a stagnant lower layer.

Hansen and Rattray point out that circulation in sea straits is similar to that in estuaries, except for the fact that one often deals with adjacent basin water masses that may be neither fresh nor truly oceanic. The Bosporus, they continue, has some similarity to a salt wedge estuary even though the salinity of the upper layer is 18 $^{o}/_{oo}$, characteristic of Black Sea surface water.

In Figure 17, I have plotted representative points on the Hansen-Rattray diagram for the Tsugaru Strait and four other straits. The results of this analysis are most encouraging.

Data for the Bosporus (Telli Bay to Madschiar Bay) and the lower Dardenelles (Erenköi Liman) were taken from the observations of Merz (Möller, 1928). In the Bosporus, the outflowing Black Sea water flows over a wedge-shaped intrusion of Aegean Sea water (see Defant, 1961, Fig. 241), reminiscent of a salt wedge estuary. In the H-R diagram, the

SYMBOL	STRAIT	SOURCE
B	BOSPORUS	Möller (1928)
D	LOWER DARDANELLES	Möller (1928)
BM	BAB-EL-MANDEB	Vercelli (1929)
G	GIBRALTAR	Schott (1928)
T	TSUGARU	This paper

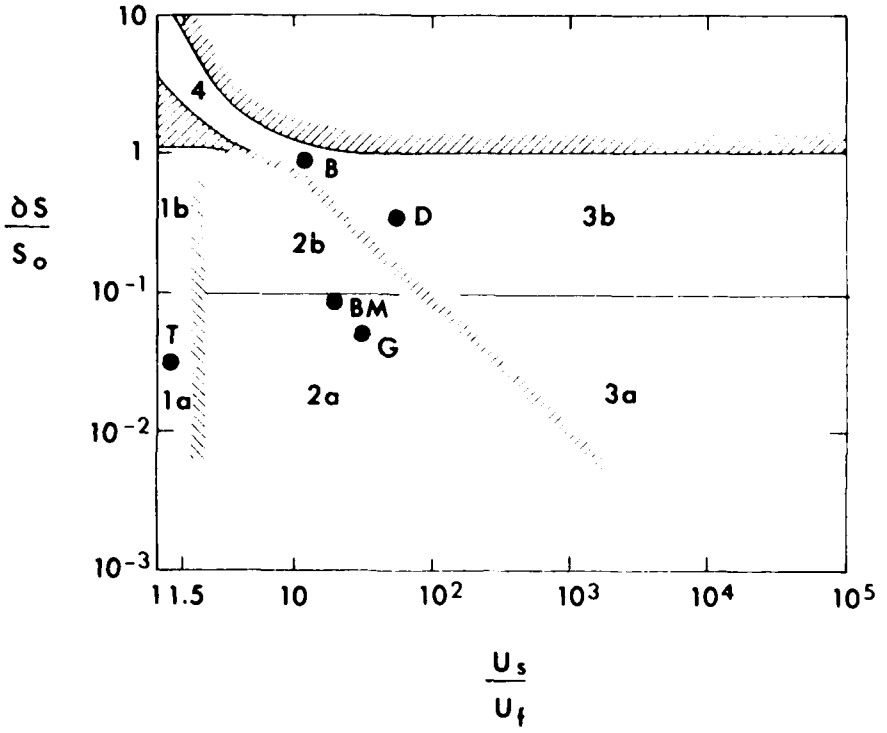

Figure 17. The Hansen-Rattray (1966) estuarine classification diagram applied to various sea straits. See text for explanation of classification parameters.

Bosporus appears as near a salt wedge state. In the lower reaches of the Dardanelles, however, a thin, high-speed layer of Black Sea origin flows over a deep and comparatively sluggish lower layer, reminiscent of a fjord. The gradation of conditions between the Bosporus and the Dardanelles has a distinct similarity to the Type 4 to Type 3 transition described by Hansen and Rattray.

The points plotted for Gibraltar and Bab-el-Mandeb indicate that these straits should be dynamically similar. As Type 2a straits, a reversal of flow with depth occurs and salinity stratification is small. (Strong northerly monsoonal winds often generate a three-layered flow in Bab-el-Mandeb.) From their positions in the diagram, it can be inferred that advection and diffusion are of approximately equal importance in the salt flux balance. It might be questionable, therefore, whether it

is appropriate to apply Knudsen's Hydrographical Theorem to these straits, because the Theorem assumes a purely advective salt balance. Some previous conclusions about transport in Gibraltar based on Knudsen's relations might bear reexamination (e.g., Sverdrup et al., 1942, quoting the work of others).

The Tsugaru Strait, on the other hand, plots as a well-mixed estuary on the H-R diagram. Although the salinity stratification in the strait is not terribly different from Gibraltar or Bab-el-Mandeb, the enormous Tsushima Current influx produces a sectional mean velocity U_f that is large enough to place the strait in a Type 1 classification. Type 1 estuaries have net flow seaward at all depths, which is what we see in the Tsugaru Strait. Also, it should not be surprising that if $\partial\rho/\partial x$ is constant, equation (21) reduces to the equation of a well-mixed estuary.

While the Hansen-Rattray diagram does not in itself add any new physics to straits dynamics, it appears to be a valuable tool in distinguishing dynamic characteristics of sea straits.

CHAPTER VI

THE OUTFLOW REGION OF THE TSUGARU STRAIT

A. Introduction

Hata (1975) analyzed oceanographic station data from the outflow region of the Tsugaru Strait for the years 1933-1967 and derived average values of salinity, temperature, and transport for each of the four seasons. Two distinct modes of circulation are seen (Fig. 18). During the winter months, the Tsugaru Warm Current exits the strait, turns right, and flows along the Honshu coast on a southerly course (coastal mode). In the summer and fall, however, a broad anticyclonic gyre is formed that fills most of the coastal bight bounded on the north by Hokkaido and on the west by Honshu (gyre mode). The transport charts show that the outflow is deflected around this gyre before reestablishing its southerly course. The spring months appear to be a time of transition during which neither circulation mode is well established.

Previous research on buoyant outflow (e.g., Takano, 1954; Nof, 1978a, b; Beardsley and Hart, 1978) has primarily emphasized deflection and spreading of the outflow jet. Basic considerations of the dynamics of flow on a rotating earth lead to the natural conclusion that a buoyant jet will be deflected cum sole, and most investigations substantiate such behavior. Nof (1978b), however, calculated that a buoyant jet could deflect to the left if it possessed sufficient initial vorticity at a strait outlet. Beardsley and Hart (1978) produced analytic solutions of the outflow circulation for a small class of idealized bottom topographies, and showed that a jet in a one-layer system would deflect to the right if the topography sloped downward in the offshore direction. In a two-layer system, however, the outflow jet would react to the topography of the interface, and not the bottom. If the interface sloped upward offshore, the jet would then deflect to the left instead of to the right.

None of these studies, however, addresses the crucial point of gyre formation. In that context, the work of Whitehead and Miller (1979) is unique, and it will not be described at length.

Whitehead and Miller (1979, hereafter referred to as WM) investigated the dynamics of gyre formation near sea straits in a series of laboratory experiments. WM employed two connecting basins on a 2-m rotating turntable. The basins were filled with water of different densities and initially were separated by a door. After spinning up the fluids, the door was opened and the resulting two-layer flow was examined using photographs of pellets floating on the surface.

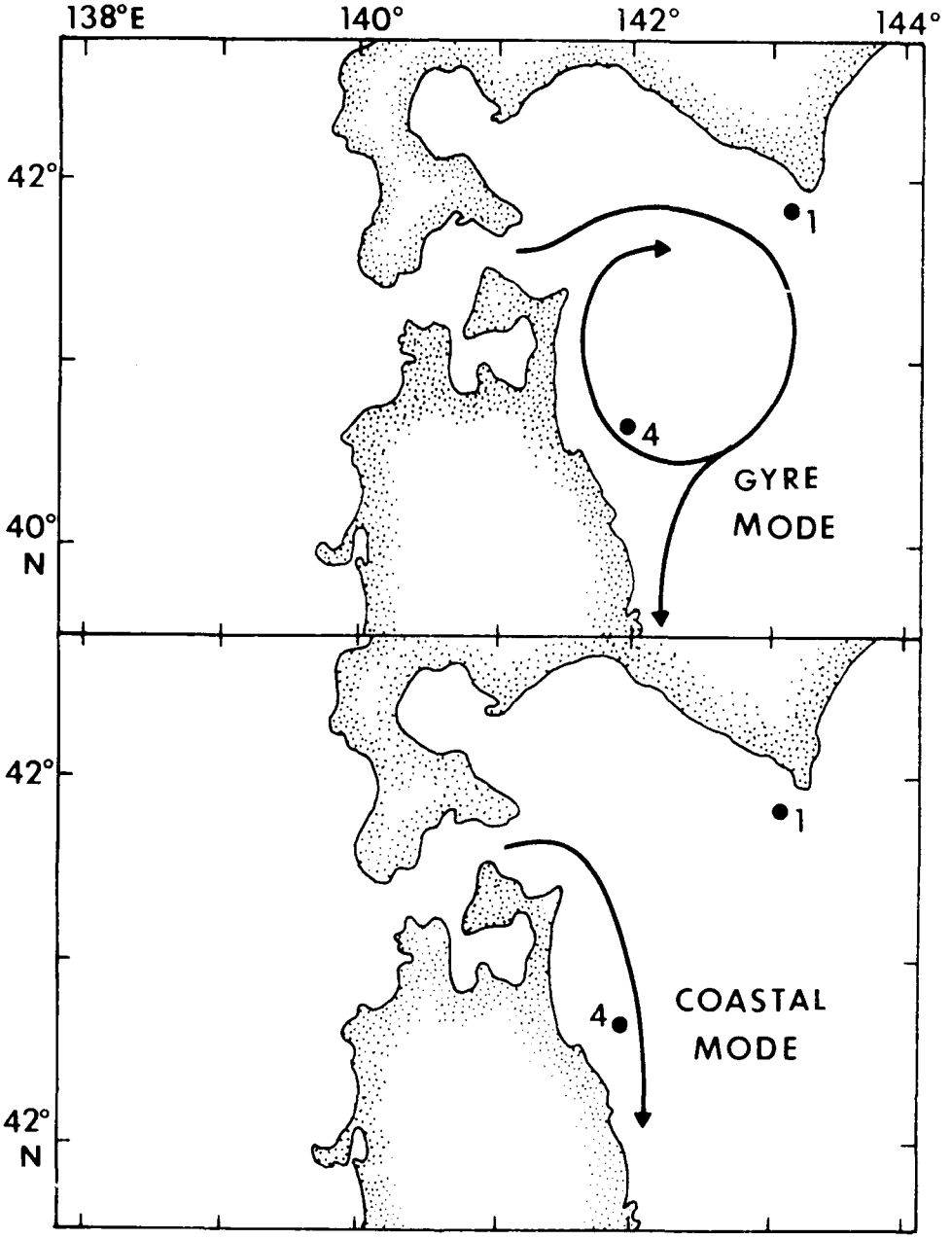

Figure 18. Schematic representation of principal modes of outflow jet from the Tsugaru Strait. Upper picture: gyre mode of warmer months. Lower picture: coastal mode of colder months. Positions of USNS SILAS BENT current moorings of November 1975-January 1976 also shown.

The natural length scale of such a density-driven process is the internal Rossby radius of deformation, $R = (g' \Delta\rho\, h/\rho f^2)^{1/2}$, which was varied in the experiments by adjusting the rotation period of the turntable.

The results of the WM experiments can be summarized as follows. When R was significantly smaller than the width of the channel (fast rotation), violent instability was generated and there was little transport between basins. As R was increased to a value greater than the width of the channel, the water from the fresh basin flowed into the salty basin as a narrow jet (close to R in width) hugging the right wall. For Rossby radii less than or equal to the radius of curvature of the channel wall, the jet remained next to the right-hand wall. When R exceeded the wall curvature, however, the jet would separate from the wall and a gyre would begin to develop. The gyre development stemmed from the separated jet impinging on the right-hand wall, at which stagnation point the jet bifurcated into a downstream component and a return flow (i.e., back toward the opening). The return flow was subsequently deflected to the right and curled around repeatedly, thus forming a gyre between the wall and the separated jet. The gyre was initially a Rossby radius in width, but grew steadily, roughly as the square root of elapsed time. In subsequent experiments, WM used a suitably scaled model of the Strait of Gibraltar to investigate the gyre observed in the Alboran Sea. Initially the flow from the "Atlantic" basin veered southward toward the African coast. The jet soon separated, producing a stagnation point at a location corresponding to Cape Tres Forcas. A gyre developed and gradually occupied the entire western Alboran Basin. The inflow jet, which initially veered south, was progressively diverted toward the north, ultimately appearing as a northward-deflected jet hugging the coast of Spain. In all respects, the characteristics of the Alboran gyre were accurately scaled, but perhaps the most significant result of WM was the demonstration that the coastal mode and gyre mode are members of a continuum of outflow modes that can be generated by altering the Rossby radius.

B. Temporal Variability of Tsugaru Warm Current

A comparison of the results of WM to the Tsugaru Strait region first requires a determination of the seasonal variability of the internal Rossby radius of the Tsugaru Warm Current.

I obtained the monthly variability of the upper-layer density of the current from data gathered by the RMS OYASHIO MARU in 97 transects run eastward from the Honshu coast at latitude 40°32.5' north during the years 1949-1957. The station at longitude 142° east is central to the flow regimes of both coastal and gyre modes (Fig. 18); measurements at the 2-km level were used in order to avoid transient surface effects. The underlying water in this region is of Oyashio origin and is stable throughout the year; the transition to this lower layer occurs at the σ_t = 26.5 isopycnal (Sugiura, 1958), from which we calculate g'.

Hata's (1975) analysis produced estimates of the upper layer thickness of 180 m during the cold months and 240 m during late summer

and fall. Because the Rossby radius varies as $h^{1/2}$, a general estimate of 210 m for the depth of the surface layer should then be adequate within about 10%.

Using these results, I calculated estimates of the monthly variation of the internal Rossby radius (Table 5). Comparison of these numbers with Hata's (1975) results appears to indicate that R values of less than 10 km represent the coastal mode, while the gyre mode is established when R exceeds 15 km.

The exact value of a "critical" Rossby radius remains unclear. WM point out that the critical Rossby radius could be a function of the width of the strait at the outlet, Ekman number, or sidewall topography. The width of the Tsugaru Strait at Ohata is about 18 km, an encouraging value, but the width increases sharply shortly thereafter. The significance of the fingerlike shelf protruding north of Shiriya Saki is unclear (Fig. 13). Of greater promise dynamically is the eastern continental shelf of Honshu. At about latitude 41° north, the width of the shelf (denoted by the 200-m isobath) increases abruptly. Also, an examination of several examples of Tsugaru Warm Current gyres reveals that the stagnation point is rather stably located at a point on or near the continental shelf ESE of Hachinohe. Whether this shelf bulge acts as a stagnation point deflector (WM) is a question that must await further investigation.

C. The Transition from Gyre Mode to Coastal Mode

From the values given in Table 5, we see that the mean Rossby radius drops abruptly in December-January from 14.2 km to 8.2 km.

Table 5
Seasonal Variation of Internal Rossby Radius

	Upper Density Layer (σ_τ)*	Rossby Radius (Est.)** (km)
January	26.2	8.2
February	26.4	4.7
March	26.4	4.7
April	26.3	6.7
May	26.0	10.6
June	25.8	12.5
July	25.0	18.4
August	24.1	23.2
September	24.0	23.7
October	24.2	22.7
November	25.1	17.7
December	25.6	14.2

*From surveys of RMS OYASHIO MARU, 1949-1952.
**Based on lower layer density of σ_τ = 26.5 (Sugiura, 1958) and upper layer mean thickness of 210 m (Hata, 1975)

The analysis presented above indicated that the outflow jet should undergo a transition from gyre mode to jet mode during this period.

In this section I will examine a transition observed during late 1975 and early 1976.

Data from a survey conducted on the KOFU MARU and SHUMPU MARU in October 1975 are displayed in Figure 19. Contours of temperature and salinity at 100 m clearly show an anticyclonic warm core gyre typical of the fall season. The surface GEK measurements further show that the outflow jet is initially deflected to the left, then moves in a clockwise arc out to longitude 143° east, turns back toward the coast at latitude 41° north, and then bifurcates near 40°30'N, 142°E. The Rossby radius of the jet can be approximated from the hydrographic data; density difference $\Delta\rho = 2.5 \times 10^{-3}$ and depth of mixed layer h = 250 m give a figure of R ~ 25 km. Sectional profiles of T, S, and ρ suggest that the jet is between 20 km and 40 km wide, which is in rough agreement with the theoretical value.

By late February 1976 the picture has changed completely (Fig. 20). The anticyclonic gyre has disappeared, and now the flow is in the coastal mode.

Figure 21 depicts 72-hour averaged currents obtained from current meters deployed by the USNS SILAS BENT during the period November 1975 to January 1976. Current meter 1 (northern location) shows weak currents of about 20 cm/sec or less, but the direction of the current is remarkably uniform from the beginning of the record until about December 19. The direction of the current (320°-340°) and its clear steadiness indicate the presence of a coastal countercurrent generated by the steady infilling of the adjacent bight by the Tsugaru Warm Current gyre.

Current meter 4, on the other hand, is located within the zone of influence of both gyre mode and coastal mode. From November 17 to November 25, the currents are strong (up to 1 knot) and very steady on a bearing of 20°, which indicates that the gyre is still active. The period between November 27 and December 14 appears to be a time of instability. The direction alternates from roughly southerly (November 27-December 4) to near northerly (around December 10) to easterly (December 14), with a trend toward decreasing current speeds. Sometime on December 15 or 16, however, the current speed picks up sharply, and the direction swings to the south, remaining between about 140° and 200° for the remainder of the record. It is clear that the coastal mode has been firmly established.

A maximum estimate of the time of transition in this case is about 3 weeks (November 25-December 15). The close agreement between the abrupt direction changes at locations 1 and 4, however, indicate that the actual transition might be very rapid (order of days instead of weeks).

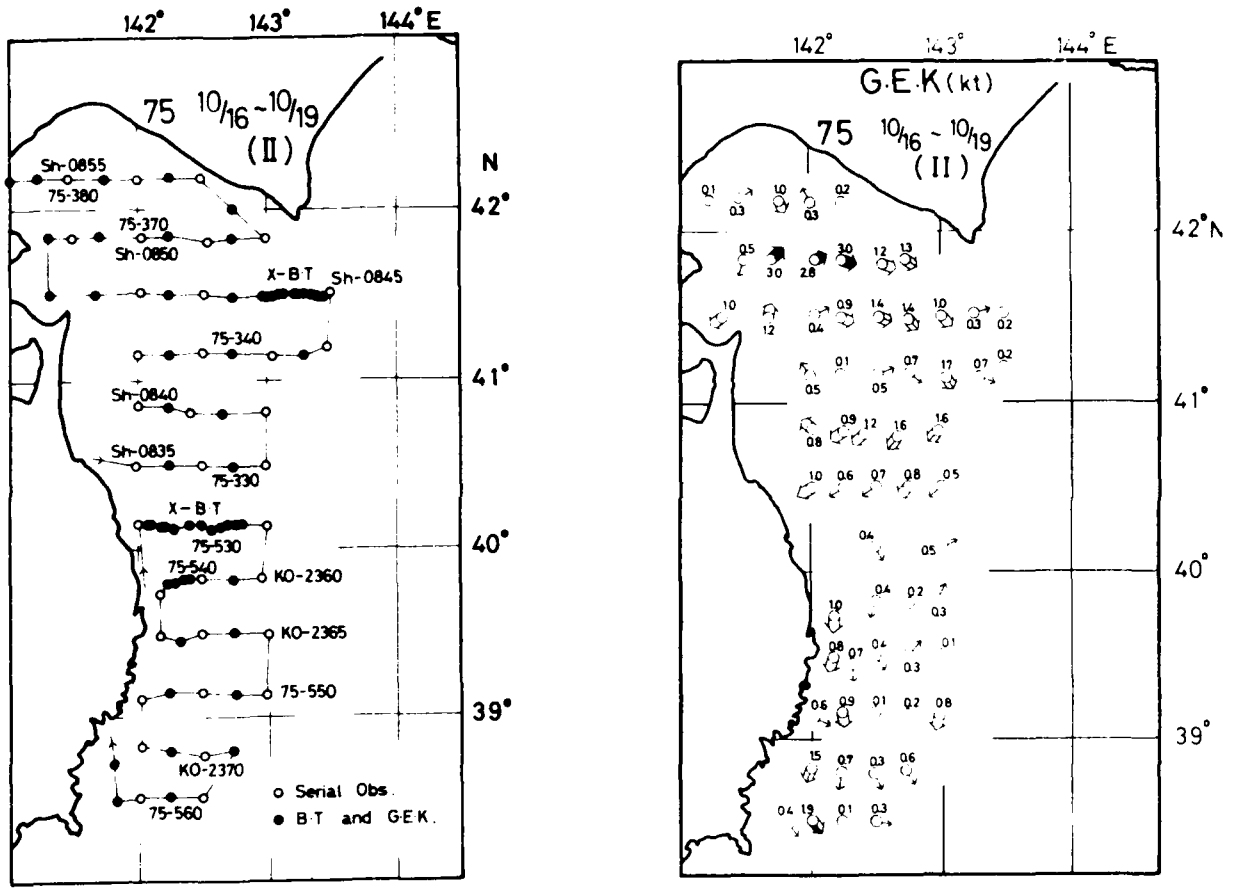

Figure 19. The outflow region of the Tsugaru Strait in October 1975, during cruises of KORU MARU and SHUMPU MARU. T_{100} and GEK data show presence of anticyclonic gyre. (Hakodate Marine Observatory, Oceanographic Observation Report, Vol. 13, No. 4.)

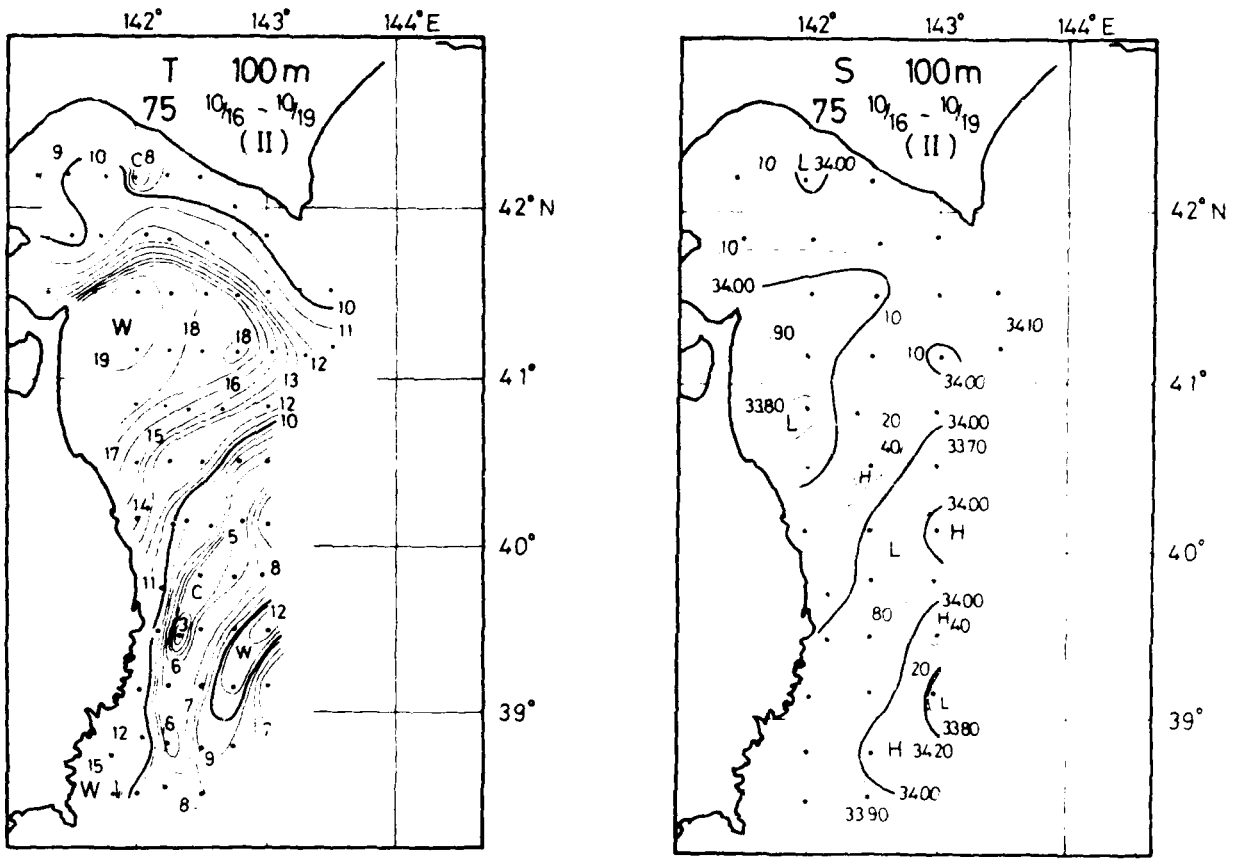

Figure 19 continued.

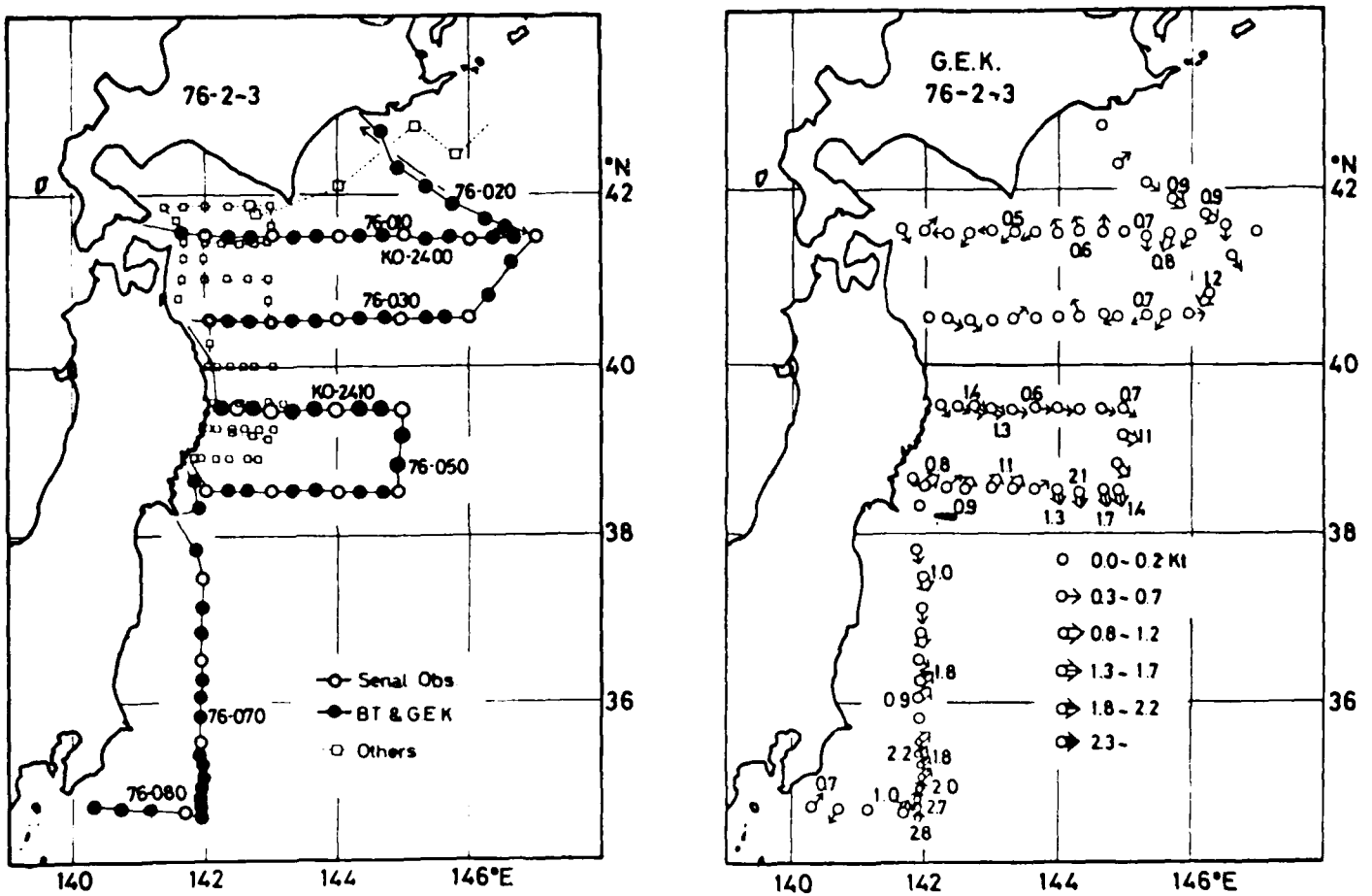

Figure 20. The outflow region of the Tsugaru Strait in February-March 1976, during cruise of KOFU MARU. T_{100} and S_{100} indicate coastal mode of outflow. (Hakodate Marine Oberva-tory, Oceanographic Observation Report, Vol. 14, No. 1.)

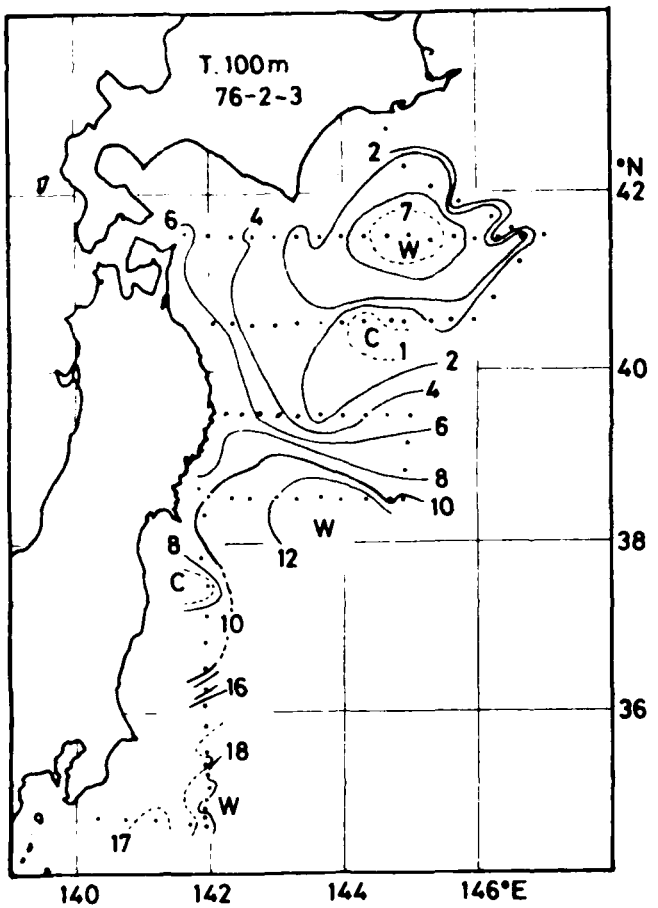

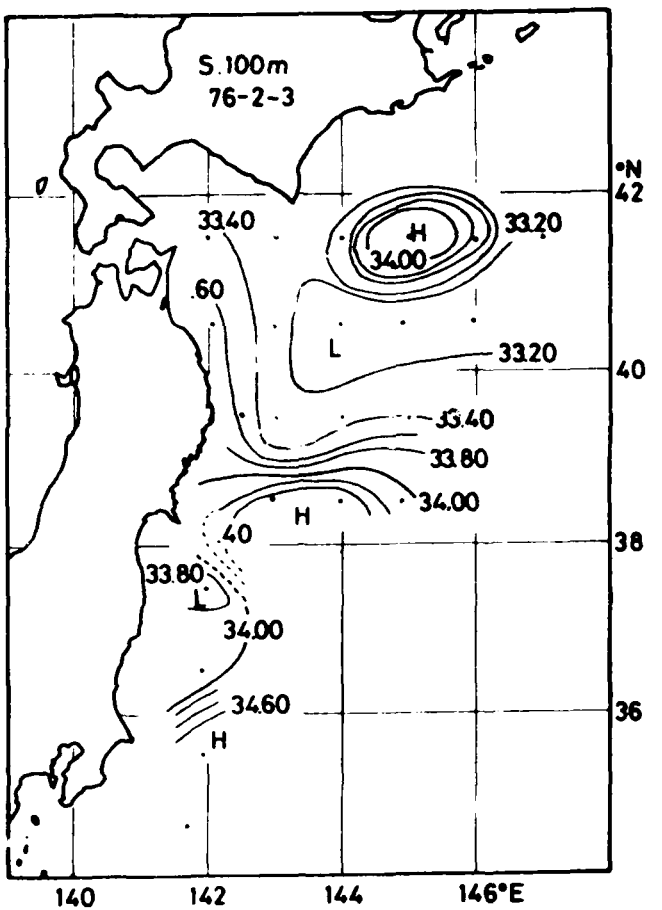

Figure 20 continued.

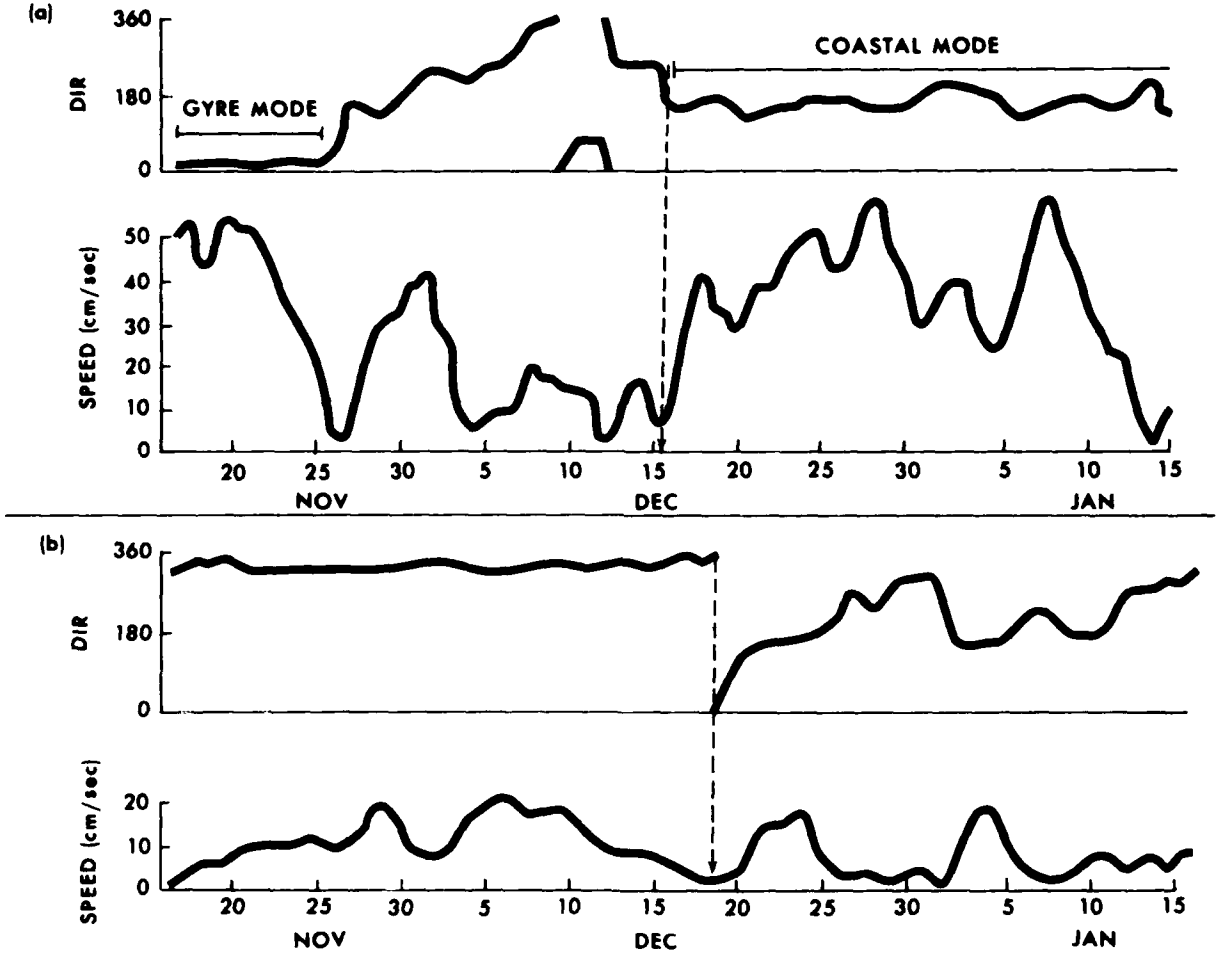

Figure 21. Currents in the outflow region of the Tsugaru Strait, November 1975-January 1976, from survey of USNS SILAS BENT. Current data have been averaged by 72-hour running mean. (a) Southern location, position 4, 45-m depth (see Fig. 15). (b) Northern location, position 1, 115-m depth.

CHAPTER VII

SUMMARY AND CONCLUSIONS

A study of the dynamics of flow in the Tsugaru Strait region reveals that the strait must be treated in the context of regional oceanographic processes as a whole. In the inflow region, processes are governed by the Tsushima Current, a part of the Kuroshio system of currents. Within the strait, the Tsushima Current influx is so large that "normal" two-layer exchange is eliminated. The dynamics of the outflow jet (Tsugaru Warm Current) are significantly affected by the characteristics of the water entering the Sea of Japan through the Korea Strait. In order to gain a more complete understanding of the dynamics of the Tsugaru Strait, it will therefore be necessary to consider processes on a much larger scale than is treated in this thesis.

Major conclusions of this work are as follows:

1. The Tsushima Current is in geostrophic balance in the cross-stream direction as it approaches the Tsugaru Strait. The baroclinic part of the Tsushima Current is principally confined to the upper 200 m of the water column, and the barotropic part appears to be of second-order importance.

2. Steric sea leveling in the inflow region shows that setup induced by the Tsushima Current decreases sharply in the vicinity of the Tsugaru Strait. The northward drop in coastal sea level is balanced by a diversion of Tsushima Current volume transport into the strait; i.e., the forcing of flow into the strait is chiefly barotropic.

3. Steric and geodetic leveling calculations indicate that sea level in the Japan Sea is lower than that in the adjacent North Pacific Ocean. This implies that the barotropic forcing of eastward flow thrugh the Tsugaru Strait is dependent on the forcing of the Tsushima Current, an understanding of which requires a study of the dynamics of the Kuroshio itself.

4. The principal balance in the longstream momentum equation for the strait is between the barotropic pressure gradient (sea level drop along the strait), the longitudinal baroclinic pressure gradient, and friction. At low to moderate wind speeds, wind stress appears to be of second-order significance, but available data are not sufficient to state this conclusion firmly. Still less well known is the effect of lateral friction, which is probably not significant within the strait current core but which must be important in the regions of sidewall eddies.

5. In the central region of the strait, currents typically do not reverse in direction with depth or in time, despite the existence of strong tidal forcing. This phenomenon is due to the massive influx of water from the Tsushima Current, which produces conditions similar to those of a well-mixed estuary, a conclusion that is supported by the circulation-stratification estuarine classification diagram of Hansen and Rattray (1966).

6. The outflow from the Tsugaru Strait into the North Pacific Ocean displays two principal modes of circulation--a coastal mode (colder months) and a gyre mode (warmer months)--the existence of which appears to depend on the value of the internal deformation radius, a result that is consistent with the laboratory findings of Whitehead and Miller (1979).

7. Field data obtained in the outflow region in October 1975-February 1976 indicate that a transition from gyre mode to jet mode took place in a period of at most 3 weeks, and possibly only several days.

REFERENCES

Beardsley, R. C., and J. Hart, 1978, A simple model for the flow of an estuary onto a continental shelf. J. Geophys. Res., 53(C2), pp. 873-883.

Defant, A., 1930, Die Bewegungen und der thermo-haline Aufbau der Wassermassen im Meeresstrassen. Sitzungsber. Preuss. Akad. Wiss., Phys.-Math. Klasse (Berlin), pp. 191-208.

Defant, A., 1961, Physical oceanography. Volume 1, New York (Pergamon).

Fukuoka, J., 1957, On the Tsushima Current. J. Oceanogr. Soc. Japan, 13(2):57-60.

Hamano, S., 1977, Short-period variation of the surface temperature in the Tsugaru Straits. Bull. Hakodate Mar. Observ., 19:1-9 (in Japanese).

Hansen, D. V., and M. Rattray, Jr., 1966, New dimensions in estuary classification. Limnol. Oceanogr., 11(3):319-326.

Hata, K., 1962, Seasonal variations of the volume transport in the northern part of the Japan Sea. J. Oceanogr. Soc. Japan, 20th Anniv. Vol., pp. 168-179 (in Japanese).

Hata, K., 1975, Variations in hydrographic conditions in the seas adjacent to the Tsugaru Straits. Bull. Hakodate Mar. Observ., 18:17-29 (in Japanese).

Hata, K., S. Hosoda, and K. Yamamoto, 1964, Report of the detailed oceanographic observations in the Tsugaru Straits from August to September, 1962. Bull. Hakodate Mar. Observ., Special Number, pp. 1-30 (in Japanese).

Hidaka, K., 1956, Computation of the wind stresses over the ocean. Rec. Oceanogr. Works Japan (new series), 4(2):77-123.

Hidaka, K., 1966, Japan Sea. In (R. W. Fairbridge, ed.) The Encyclopedia of Oceanography, pp. 417-424.

Hikosaka, S., 1953, On the ocean-currents (non-tidal currents) in the Tsugaru Strait. Hydrogr. Bull., 39:279-285 (in Japanese).

Iida, H., 1972, On the shape of the sea surface along the coast of islands of Japan. Oceanogr. Mag., 23:69-79.

Japan Meteorological Agency, 1972, The results of marine meteorological and oceanographical observations. Vol. 48.

Kitano, K., 1975, Some properties of the warm eddies generated in the confluence zone of the Kuroshio and Oyashio Currents. J. Phys. Oceanogr., 5:245-252.

Lisitzin, E., 1965, The mean sea level of the world ocean. Soc. Sci. Fennica, Comm. Phys. Math., 30(7), 35 pp.

Lisitzin, E., 1967, Sea level variation in the Sea of Japan. Int. Hydrogr. Rev., 44(2):11-22.

Miyazaki, Ma., 1955, Seasonal variations of the sea level along the Japanese coasts. Rec. Oceanogr. Works Japan (new series), 2(3): 1-8.

Miyazaki, Mi., 1952, The heat budget in the Japan Sea. Rep. Hokkaido Reg. Fisher. Res. Lab., 4:1-45 (in Japanese).

Möller, L., 1928, Alfred Merz' hydrographische Untersuchungen in Bosporus und Dardanellen. Veröff. Inst. f. Meeresk., Reihe A, 18.

Montgomery, R. B., 1969, Comments on oceanic leveling. Deep-Sea Res., 16 (Supplement):147-152.

Moriyasu, S., 1972, The Tsushima Current. In (*H. Stommel and K. Yoshida*, eds.) Kuroshio: Physical Aspects of the Japan Current, Seattle (Univ. Washington Press), pp. 353-369.

Nan-niti, T., H. Akamatsu, and T. Yasuoka, 1966, A deep current measurement in the Japan Sea. Oceanogr. Mag., 18:(1-2):63-71.

Nof, D., 1978a, On geostrophic adjustment in sea straits and wide estuaries: theory and laboratory experiments. Part I, One-layer system. J. Phys. Oceanogr., 8:690-702.

Nof, D., 1978b, On geostrophic adjustment in sea straits and wide estuaries: theory and laboratory experiments. Part II, Two-layer system. J. Phys. Oceanogr., 8:861-872.

Nomitsu, T., and M. Okamoto, 1927, The causes of the annual variation of the mean sea level along the Japanese coast. Mem. Coll. Sci. Kyoto (A), 10(3):125-161.

Officer, C. B., 1976, Physical oceanography of estuaries (and associated coastal waters). New York (John Wiley).

Ogura, S., 1933, The tides in the seas adjacent to Japan. Bull. Hydrogr. Dept. Imp. Japan Navy, 7.

Ohwada, M., and K. Tanioka, 1972, Cruise report on the simultaneous observation of the Japan Sea in October 1969. Oceanogr. Mag., 23:47-58.

Patullo, J., W. Munk, R. Revelle, and E. Strong, 1955, The seasonal oscillation in sea level. J. Mar. Res., 14(1):88-113.

Pond, S., and G. L. Pickard, 1978, Introductory dynamic oceanography. New York (Pergamon).

Reid, J. L., and A. Mantyla, 1976, The effect of geostrophic flow upon coastal sea elevations in the northern North Pacific Ocean. J. Geophys. Res., 81(18):3100-3110.

Schott, G., 1928, Die Wasserbewegungen im Gebiete der Gibraltarstrasse. J. Cons. Intern., 3(2).

Science and Technology Agency, 1972, Report on comprehensive investigations of the Sea of Japan, 1970. (In Japanese.)

Science and Technology Agency, 1979, Report on the comprehensive investigations in the Tsugaru Strait, 1975-77. (In Japanese).

Sturges, W., 1967, Slope of sea level along the Pacific coast of the United States. J. Geophys. Res., 72(14):3627-3637.

Sturges, W., 1968, Sea-surface topography near the Gulf Stream. Deep-Sea Res., 15:149-156.

Sturges, W., 1974, Sea level slope along continental boundaries. J. Geophys. Res., 79(6):825-830.

Suda, K., K. Hidaka, Y. Matudaira, H. Kawasaki, T. Takahata, T. Kubo, and Z. Yasui, 1932, Report on the oceanographical observations on board the R.M.S. "Shumpu Maru" in Tsugaru Strait. J. Oceanogr. Kobe Imp. Mar. Observ., 4(2):341-357.

Sugiura, J., 1958, On the Tsugaru Warm Current. Geophys. Mag., 28:399-409.

Sverdrup, H. U., M. W. Johnson, and R. H. Fleming, 1942, The oceans. Englewood Cliffs (Prentice-Hall).

Takano, K., 1954, On the velocity distribution off the mouth of a river. J. Oceanogr. Soc. Japan, 10:60-64.

Tanioka, J., 1968, On the Eastern Korean Warm Current (Tosen Warm Current). Oceanogr. Mag., 20(1):31-38.

Uda, M., 1934, Hydrographical studies based on simultaneous oceanographical surveys made in the Japan Sea and its adjacent waters during May and June, 1932. Rec. Oceanogr. Works Japan, 6(1):19-107.

Vercelli, F., 1928, Nuove recherche sulli correnti marine del Mar Rosso. Annali Idrogr., 12:1-74.

Whitehead, J. A., and A. R. Miller, 1979, Laboratory simulation of the gyre in the Alboran Sea. J. Geophys Res., 84(C7):3733-3742.

Yasui, M., T. Yasuoka, K. Tanioka, and O. Shiota, 1967, Oceanographic studies of the Japan Sea, (1) Water characteristics. Oceanogr. Mag., 19(2):177-192.

Yi, S.-U., 1967, Seasonal variation of monthly sea level along the coast of Korea. J. Oceanol. Soc. Korea, 2:24-33.

Unclassified

Security Classification

AD-A096 948

DOCUMENT CONTROL DATA - R & D

Security classification of title, body of abstract and indexing annotation must be entered when the overall report is classified.

1. ORIGINATING ACTIVITY (Corporate author) Coastal Studies Institute Louisiana State University Baton Rouge, Louisiana 70803	2a. REPORT SECURITY CLASSIFICATION Unclassified 2b. GROUP Unclassified

3. REPORT TITLE

DYNAMICS OF FLOW IN THE REGION OF THE TSUGARU STRAIT

4. DESCRIPTIVE NOTES (*Type of report and, inclusive dates*)

5. AUTHOR(S) (*First name, middle initial, last name*)

Dennis M. Conlon

6. REPORT DATE	7a. TOTAL NO. OF PAGES	7b. NO. OF REFS
March 198	62	48

8a. CONTRACT OR GRANT NO. N00014-75-C-0192 b. PROJECT NO. NR 388 002 c. d.	9a. ORIGINATOR'S REPORT NUMBER(S) Coastal Studies Institute Technical Report 312 9b. OTHER REPORT NO(S) (*Any other numbers that may be assigned this report*) SSR-1

10. DISTRIBUTION STATEMENT

Approved for public release; distribution unlimited.

11. SUPPLEMENTARY NOTES	12. SPONSORING MILITARY ACTIVITY Coastal Sciences Program Office of Naval Research Arlington, Virginia 22217

13. ABSTRACT

The Tsugaru Strait is one of four straits that connect the Sea of Japan to adjacent oceans. Flow dynamics in the Tsugaru Strait region are closely tied to the dynamics of the Tsushima Current, a branch of the Kuroshio that enters the Sea of Japan through the Korea Strait and exits through the Tsugaru and Soya Straits. This research concentrates on the dynamic interplay of the Tsushima Current and the Tsugaru Strait in three regions: the inflow region (Sea of Japan side), the strait itself, and the outflow region (North Pacific side). (U)

Dynamic calculations and steric sea leveling in the inflow region indicate that transport into the Tsugaru Strait is principally governed by the geostrophically balanced Tsushima Current. Setup generated south of the strait by the Tsushima Current cannot be maintained at the entrance to the strait; the resulting northward drop in coastal sea level is balanced by a net loss of transport into the strait. Within the strait, the flow is geostrophically balanced in the cross-stream direction. In the longstream direction, the barotropic pressure gradient is chiefly balanced by the longitudinal baroclinic pressure gradient and friction. Application of the Hansen-Rattray (1966) estuarine classification scheme to several straits shows that the Tsugaru Strait displays dynamics similar to that of a well-mixed estuary. The outflow jet emerging from the eastern mouth of the strait is governed by inertial-rotational dynamics; two distinct circulation modes, which behave in a manner consistent with the laboratory findings of Whitehead and Miller (1979), are seen. (U)

DD FORM 1473 (PAGE 1)

S/N 0102-014-6601

Unclassified

Security Classification

A-31408

14 KEY WORDS	LINK A		LINK B		LINK C	
	ROLE	WT	ROLE	WT	ROLE	WT
Flow dynamics						
Tsugaru Strait						
Steric sea leveling						
Estuarine classification scheme						

Unclassified Distribution List
Reports of Contract N00014-75-C-0102
Project NR 388 002

Office of Naval Research
Coastal Sciences Program
Code 462
Arlington, Virginia 22217

Defense Documentation Center
Cameron Station
Alexandria, Virginia 22314

Director, Naval Research Lab
Attn: Technical Information Officer
Washington, D. C. 20375

Director
Office of Naval Research
Branch Office
1030 East Green Street
Pasadena, California 91101

Director, Code 100
Office of Naval Research
Branch Office
536 South Clark Street
Chicago, Illinois 60605

Director
Office of Naval Research
Branch Office
495 Summer Street
Boston, Massachusetts 02210

Commanding Officer
Office of Naval Research
Branch Office
Box 39
FPO New York 09510

Chief of Naval Research
Asst. for Marine Corps Matters
Code 100M
Office of Naval Research
Arlington, Virginia 22217

Office of Naval Research
Code 480
National Space Technology Lab
Bay St. Louis, MS 39520

Office of Naval Research
Operational Applications Division
Code 200
Arlington, Virginia 22217

Office of Naval Research
Scientific Liaison Officer
Scripps Inst. of Oceanography
La Jolla, California 92038

Director, Naval Research Lab
Attn: Library, Code 2628
Washington, D. C. 20375

Commander
Attn: Library
NSTL Station
Bay St. Louis, MS 39520

ONR Scientific Liaison Group
American Embassy, Room A-407
APO San Francisco 96503

Chief of Naval Operations
OP 987P1
Department of the Navy
Washington, D. C. 20350

Oceanographer of the Navy
Hoffman II Building
200 Stovall Street
Alexandria, Virginia 22322

Naval Academy Library
U.S. Naval Academy
Annapolis, Maryland 21402

Commanding Officer
Naval Coastal Systems Laboratory
Panama City, Florida 32401

Librarian
Naval Intelligence Support Center
4301 Suitland Road
Washington, D. C. 20390

Commanding Officer
Naval Air Development Center
Warminster
Johnsville, PA 18974

Naval Ordinance Lab
White Oak
Silver Spring, Maryland 20910

Commanding Officer
Naval Civil Engineering Lab
Port Hueneme, CA 93041

Officer in Charge
Environmental Prediction Research Facility
Naval Post Graduate School
Monterey, California 93940

Dr. Warren C. Thompson
Dept. of Meteorology and Oceanography
Naval Post Graduate School
Monterey, California 93940

Col. B. O. Ready, NOO8
Commander, Naval Surface Force
U. S. Atlantic Fleet
Norfolk, Virginia 23511

Commander, Amphibious Force
U.S. Pacific Fleet
Force Meteorologist
COMPHIBPAC Code 25 5
San Diego, California 92155

Commanding General
Marine Corps Development and Educational Command
Quantico, Virginia 22134

Dr. A. L. Slafkosky
Scientific Advisor
Commandant of the Marine Corps
Code MC RD-1
Washington, D. C. 20380

Defense Intelligence Agency
Central Reference Division
Code RDS-3
Washington, D. C. 20301

Director
Defense Mapping Topographic Center
Attn: Code 50200
Washington, D. C. 20315

Commanding Officer
U.S. Army Engineering Topographic Lab
Attn: ETL-ST
Fort Belvoir, Virginia 22060

Director
Coastal Engineering Research Center
U.S. Army Corps of Engineers
Kingman Building
Fort Belvoir, Virginia 22060

Chief, Wave Dynamics Division
USAE-WES
P. O. Box 631
Vicksburg, Mississippi 39180

Commandant
U.S. Coast Guard
Attn: GECV/61
Washington, D. C. 20591

Office of Research and Development
c/o DB/62
U.S. Coast Guard
Washington, D. C. 20591

National Oceanographic Data Center
c/o D764
Environmental Data Services
NOAA
Washington, D. C. 20235

Assistant Director
Research and Development
National Ocean Survey
6001 Executive Boulevard
Rockville, Maryland 20852

Central Intelligence Agency
Attn: OCR/DD-Publications
Washington, D. C. 20205

Dr. Donald Swift
Marine Geology and Geophysics Laboratory
AOML-NOAA
15 Rickenbacker Causeway
Miami, Florida 33149

Dr. Mark M. Macomber
Technical Director
DMA Aerospace Center
St. Louis, AFS, MO 63118

Ministerialdirektor
Dr. F. Weyer
Rue/FO
Bundesministerium der Verteidigung
Hardthoehe
D-5300 Bonn, WEST GERMANY

Oberregierungsrat
Dr. Ulrich
Rue/FO
Bundesministerium der Verteidigung
Hardthoehe
D-5300 Bonn, WEST GERMANY

Dr. Yoshimi Goda
Director, Wave Research Div.
Port and Harbor Research Inst.
Ministry of Transportation
3-1 Nagase, 3 Chome
Yokosuka, 239 JAPAN

Mr. Ingo Stratup
Defence Research Establishment
Osterbrogades Kaserne
DK-2100 Kobenhavn O, DENMARK

Prof. Dr. Rer. Nat. H. G. Gierloff-Emden
Institut F. Geographie
Universitaet Muenchen
Luisenstrasse 37/III
D-800 Muenchen 2, WEST GERMANY

Prof. Dr. Eugen Seibold
Geol.-Palaeontolog. Institut
Universitaet Kiel
Olshausenstrasse 40-60
D-2300 Kiel, WEST GERMANY

Dr. R. Koester
Geol.-Palaeontolog. Institut
Universitaet Kiel
Olshausenstrasse 40-60
D-2300 Kiel, WEST GERMANY

Prof. Dr. Ruehlbooter
Lehrstuhl F. Hydromechanik U. Kuestenwasserbau
Technische Hochschule Braunschweig
Beethovenstrasse 51A
D-3300 Braunschweig
WEST GERMANY

Prof. Dr. Walter Hansen
Direktor D. Institute F. Meereskunde
Universitaet Hamburg
Heimhuderstrasse 71
D-2000 Hamburg 13
WEST GERMANY

Prof. Dr. Klaus Hasselmann
Institut F. Geophysik
Universitaet Hamburg
Schlueterstrasse 22
D-2000 Hamburg 13
WEST GERMANY

Prof. Dr. Nils Jerlov
Institute for Physical Oceanography
Kobenhavns Universitet
Haraldsgade 6
DK 2200 Kobenhavn, DENMARK

Prof. Kiyoshi Horikawa
Dept. of Civil Engineering
University of Tokyo
7-3-1, Hongo, Bunkyo-ku
Tokyo 113, JAPAN

Prof. Yuji Iwagaki
Civil Engineering Department
Kyoto University
9 Shimogamo Tenbucho
Sakyo-ku
Kyoto, JAPAN

Delft Hydraulics Laboratory
P. O. Box 177, 2600 MH
Delft, NETHERLANDS

Ir. M. W. Van Batenburg
Physisch Laboratorium TNO
Oude Waalsdorper Weg 63
Den Haag, NETHERLANDS

Prof. Toshiyuki Shigemoto
Civil Engineering Department
National Defense Academy
1-10-20 Hashirimizu
Yokosuka 239, JAPAN

Mr. William T. Wheler
Telecommunication Enterprises Inc.
7430 Industrial Drive
Panama City, Florida 32405

Prof. Jan D. Isaacs
University of California A-207
Institute of Marine Research
La Jolla, California 92093

Dr. G. B. Hickman
Applied Science Technology, Inc.
19212 Plummer Drive
Germantown, Maryland 20767

Dr. Bernd M. Brennikmeyer, SJ
Department of Geology and Geophysics
Boston College
Cheatnut Hill, MA 02167

Dr. Charlie J. Sonu
Tek Marine, Inc.
41 West Santa Clara
Arcadia, California 91006

Dr. Richard A. Davis, Jr.
Department of Geology
University of South Florida
Tampa, Florida 33620

Dr. William T. Fox
Department of Geology
Williams College
Williamstown, MA 01267

Dr. Hsiang Wang
Department of Civil Engineering
Dupont Hall
University of Delaware
Newark, Delaware 19711

Dr. John T. Kuo
Henry Krumb School of Mines
Seeley W. Mudd Building
Columbia University
New York, New York 10027

Dr. Edward B. Thornton
Department of Oceanography
Naval Postgraduate School
Monterey, California 93940

Prof. C. A. M. King
Department of Geography
University of Nottingham
Nottingham, ENGLAND

Dr. Douglas L. Inman
Scripps Institution of Oceanography
La Jolla, California 92037

Dr. Omar Shemdin
Jet Propulsion Lab 183-501
4800 Oak Grove Drive
Pasadena, California 91103

Dr. Allen W. Niedoroda
Director, Coastal Research Center
University of Massachusetts
Amherst, MA 01003

Dr. William W. Wood
Department of Geosciences
Purdue University
Lafayette, Indiana 47907

Dr. John B. Southard
Department of Earth and Planetary Sciences
Massachusetts Inst. of Tech.
Cambridge, Massachusetts 02139

Dr. J. Ernest Breeding, Jr.
Department of Oceanography and Ocean Engineering
Florida Inst. of Technology
Melbourne, Florida 32901

Dr. John C. Kraft
Department of Geology
University of Delaware
Newark, Delaware 19711

Dr. Deg Nummedal
Department of Geology
Louisiana State University
Baton Rouge, Louisiana 70803

Dr. Lester A. Gerhardt
Rennselaer Polytechnic Institute
Troy, New York 12181

Mr. Fred Thomas
Environmental Research Institute
P. O. Box 618
Ann Arbor, Michigan 48107

Dr. Thomas R. Peucker
Simon Fraser University
Department of Geography
Burnaby 2, B. C., CANADA

Robert Dolan
Department of Environmental Sciences
University of Virginia
Charlottesville, VA 22903

Revised 6/30/80

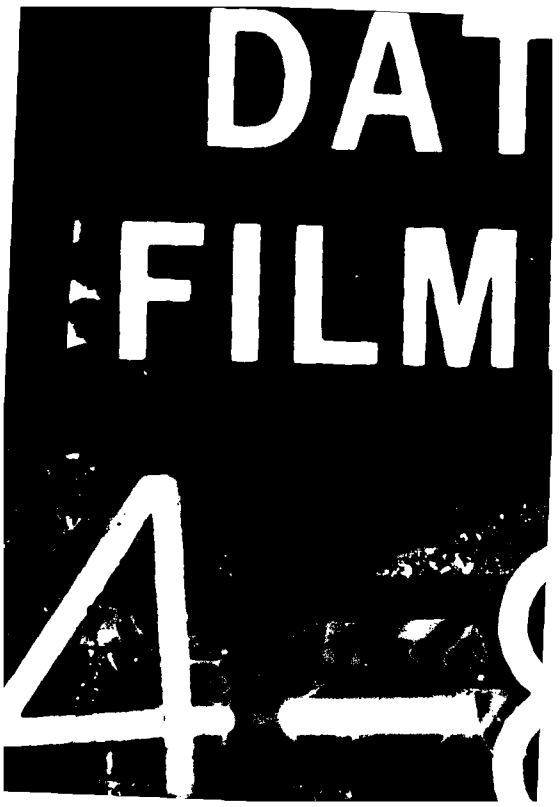
DAT
FILM